Astronomy 233   Winter 2009

Physical Cosmology
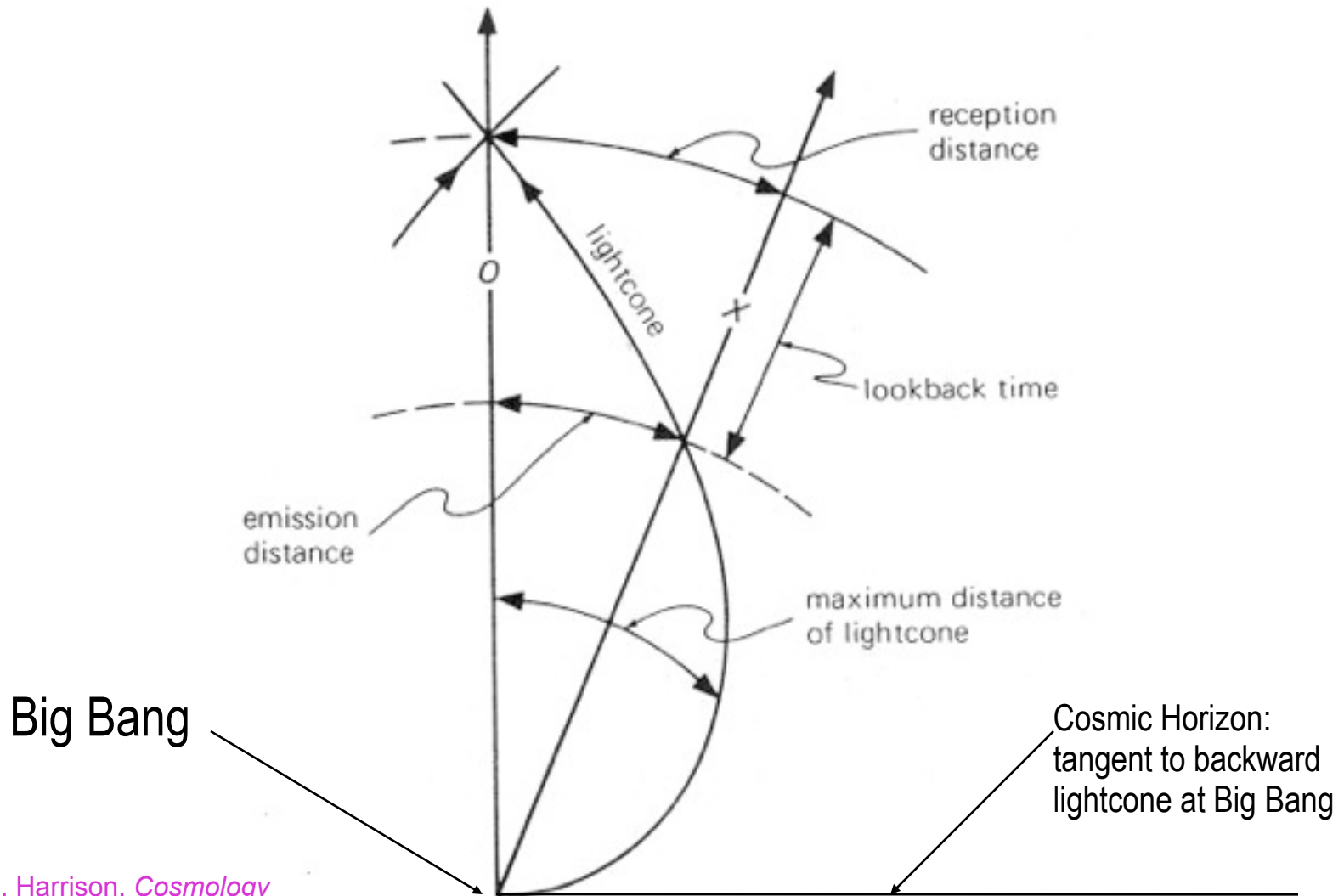
Week 4

Distances and BBN Start

Joel Primack

University of California, Santa Cruz

Picturing the History of the Universe: The Backward Lightcone

reception distance

lightcone

lookback time

O

X

emission distance

maximum distance of lightcone

Big Bang

Cosmic Horizon: tangent to backward lightcone at Big Bang

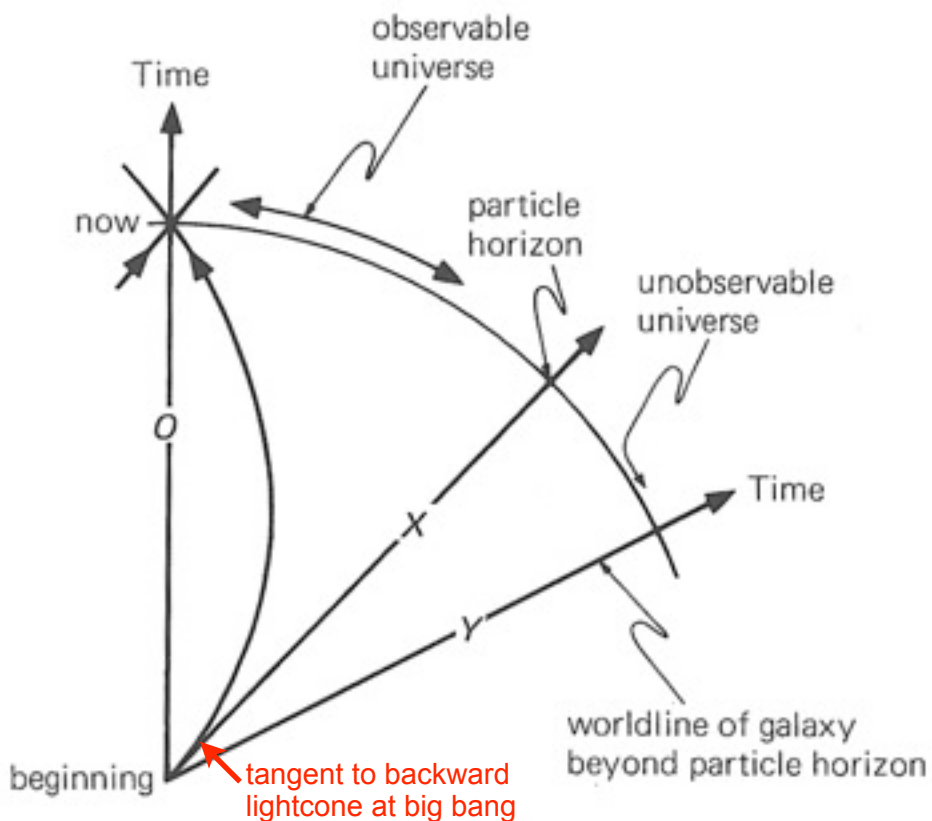# Picturing the History of the Universe: The Backward Lightcone

Figure 21.11. At the instant labeled "now" the particle horizon is at worldline X. In a big bang universe, all galaxies at the particle horizon have infinite redshift.

Labels in figure: Time; observable universe; particle horizon; unobservable universe; now; O; Time; X; Y; beginning; tangent to backward lightcone at big bang; worldline of galaxy beyond particle horizon

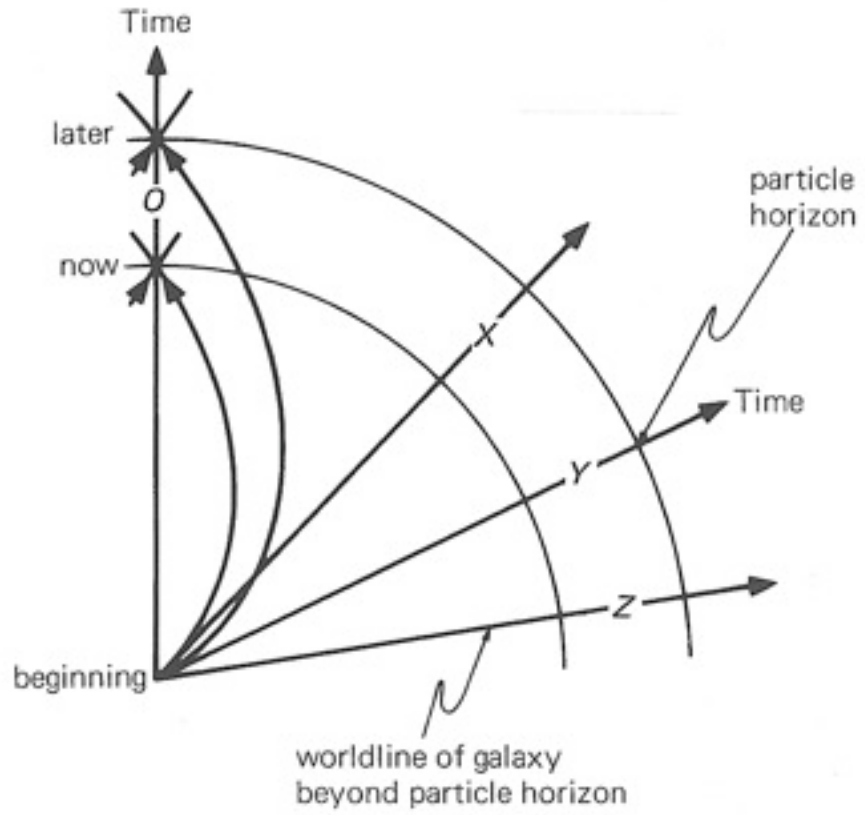From E. Harrison, *Cosmology* (Cambridge UP, 2000).

Figure 21.12. At the instant labeled "later" the particle horizon has receded to world line Y. Notice the distance of the particle horizon is always a reception distance, and the particle horizon always overtakes the galaxies and always the fraction of the universe observed increases.
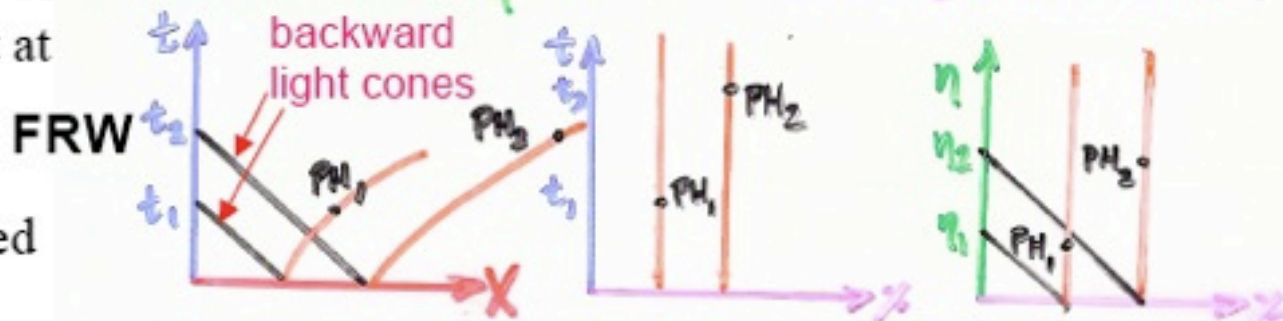
Labels in figure: Time; later; O; now; beginning; particle horizon; X; Time; Y; Z; worldline of galaxy beyond particle horizon

Horizons

PARTICLE HORIZON

Spherical surface that at time t separates *worldlines* into observed vs. unobserved

EVENT HORIZON

Backward lightcone that separates *events* that will someday be observed from those never observed

$$ds^2 = dt^2 - dX^2 = dt^2 - R^2 dx^2 = R^2(d\eta^2 - dx^2)$$

conformal time $\quad d\eta = dt/R \qquad$ comoving coord. $dx = dX/R$

FRW

backward light cones

t_2, t_1, PH_1, PH_3, t_2, t_1, PH_1, PH_2, η_2, η_1, PH_1, PH_2

deS

EH, EH, $\frac{1}{H}$, ends $\Rightarrow$ EH, EH

$$\eta = \int_{t_0}^{\infty} \frac{dt}{e^{Ht}} = \frac{1}{H} e^{-Ht_0} \leq \frac{1}{H}$$

Schwarzschild
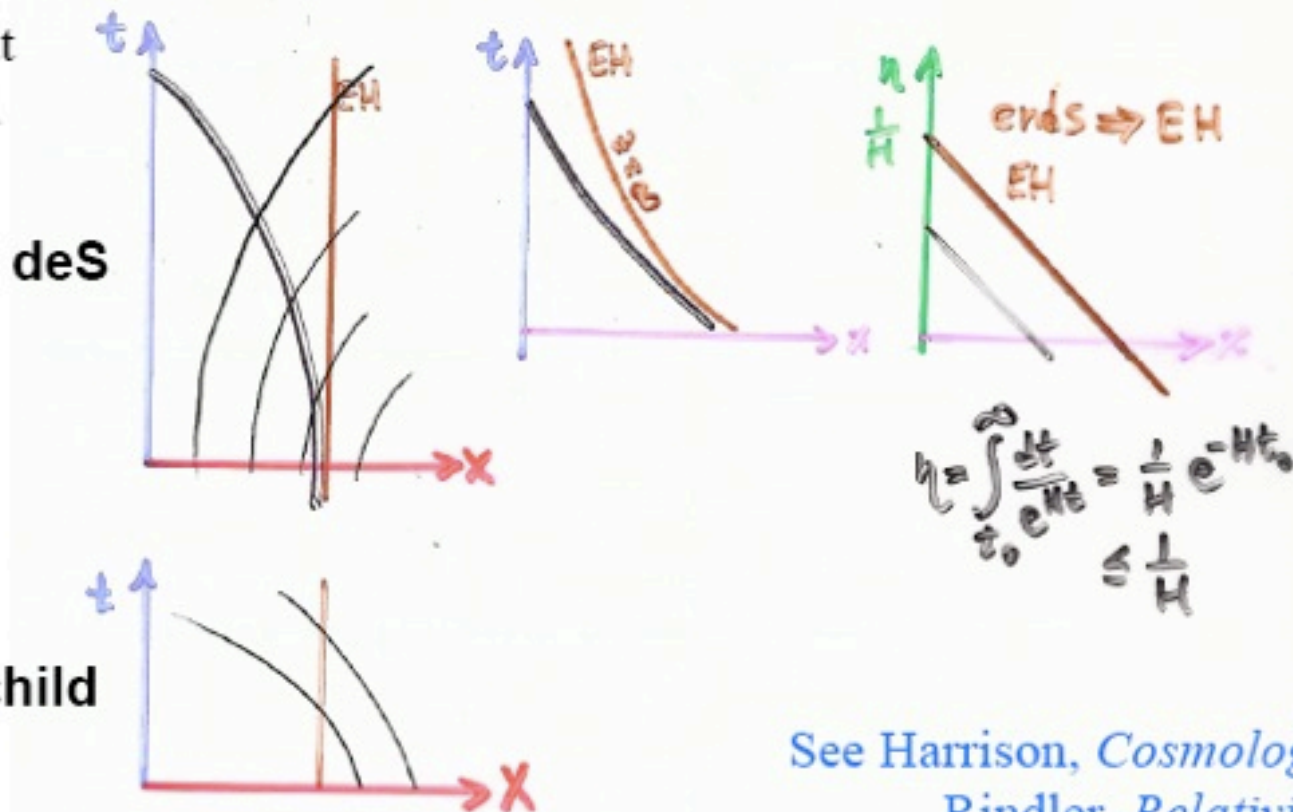
See Harrison, *Cosmology*
Rindler, *Relativity*

Distances in an Expanding Universe

Proper distance = physical distance = d_p

$d_p(t_0)$ = (physical distance at t_0) = $a(t_0)\, r_e = r_e$

$\chi(t_e)$ = (comoving distance of galaxy emitting at time t_e)

$$\chi(t_e) = \int_0^{r_e} dr = r_e = c\int_{t_e}^{t_0} dt/a = c\int_{a_e}^{1} da/(a^2 H)$$

because
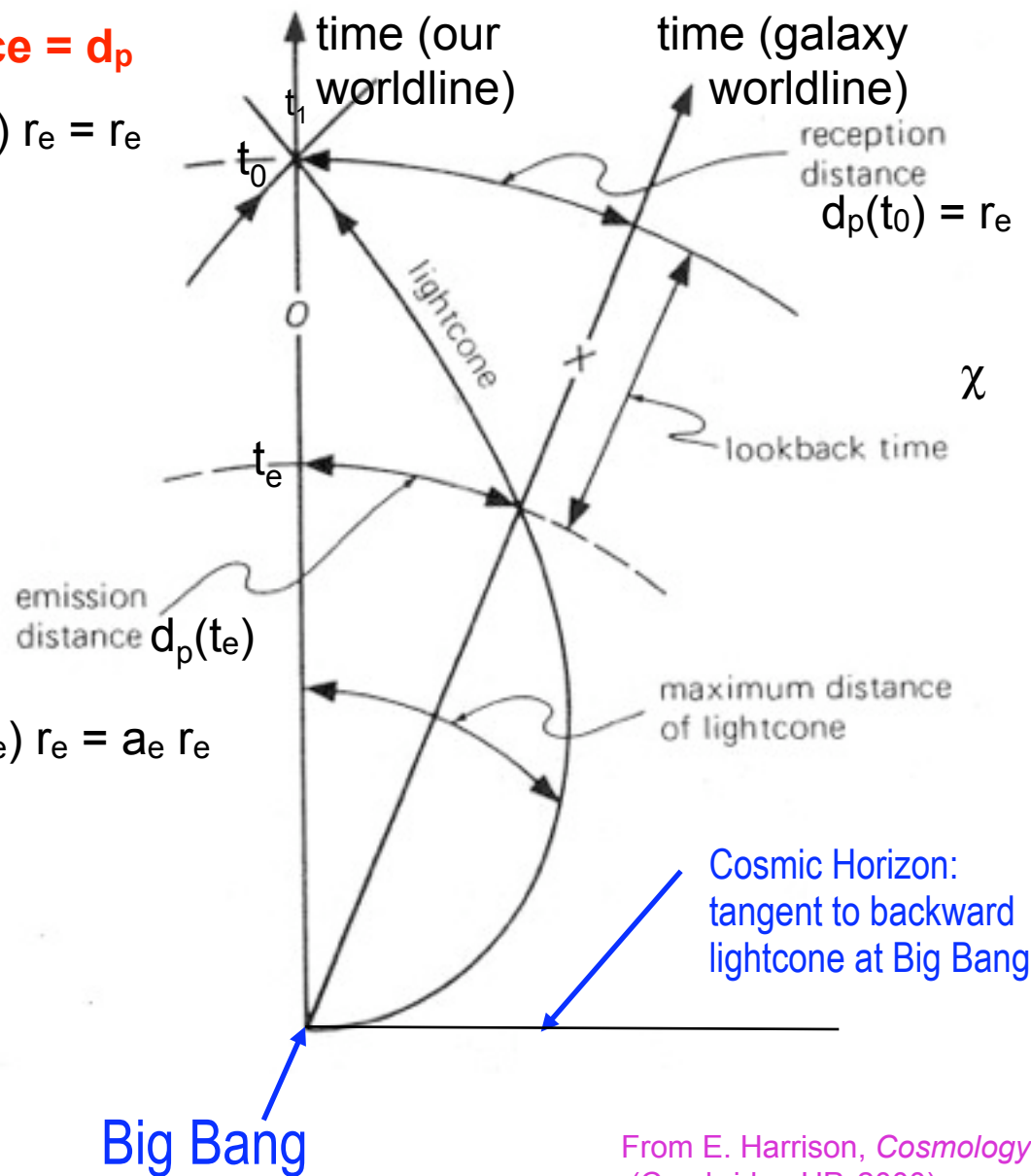
$$dt = (dt/da)\,da = (a\,dt/da)\,da/a = da/(aH)$$

$d_p(t_e)$ = (physical distance at t_e) = $a(t_e)\, r_e = a_e\, r_e$

The Hubble radius $d_H = c\,H_0^{-1}=$
$= 4.29\ h_{70}^{-1}$ Gpc $= 13.97 h_{70}^{-1}$ Glyr

For E-dS, where $H = H_0\, a^{-3/2}$,

$$\chi(t_e) = r_e = d_p(t_0) = 2d_H\,(1-a_e^{1/2})$$

$$d_p(t_e) = 2d_H\, a_e\,(1-a_e^{1/2})$$

time (our worldline)

time (galaxy worldline)

reception distance

$d_p(t_0) = r_e$

χ

lookback time

emission distance $d_p(t_e)$

maximum distance of lightcone

Cosmic Horizon: tangent to backward lightcone at Big Bang

Big Bang

From E. Harrison, *Cosmology* (Cambridge UP, 2000).

Distances in an Expanding Universe

Top plot:

observation

reception distance in units of d_H

Λ-only

Benchmark

E-dS matter-only

$\left(\frac{H_0}{c}\right) d_p(t_0)$

Hubble radius $d_H = c\,H_0^{-1} =$
$= 4.29\,h_{70}^{-1}$ Gpc
$= 13.97 h_{70}^{-1}$ Glyr

Bottom plot:

emission

emission distance in units of d_H

$\left(\frac{H_0}{c}\right) d_p(t_e)$

Λ-only

Benchmark

E-dS matter-only

z

Right diagram labels:

reception distance $d_p(t_0)$

O

lightcone

X

lookback time

$d_p(t_e)$

maximum distance of lightcone
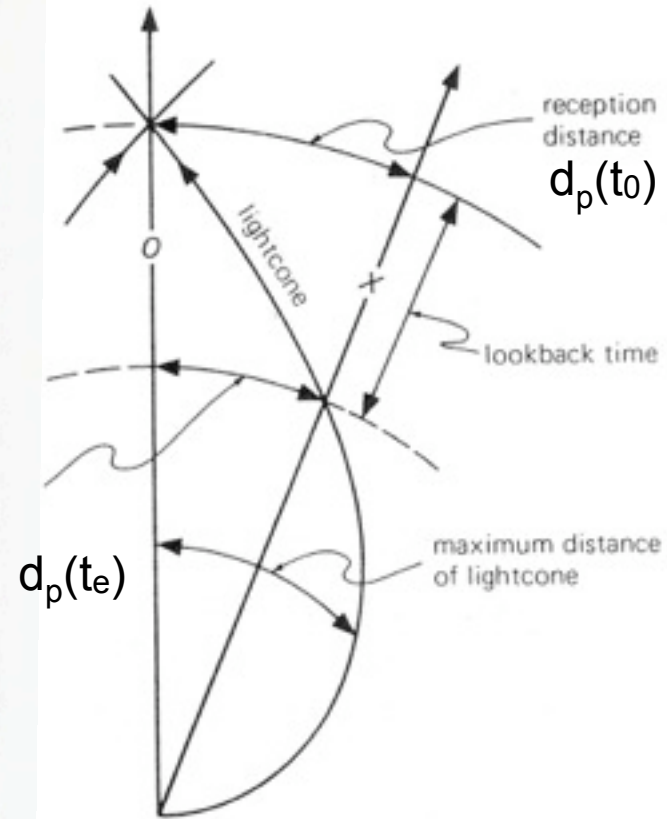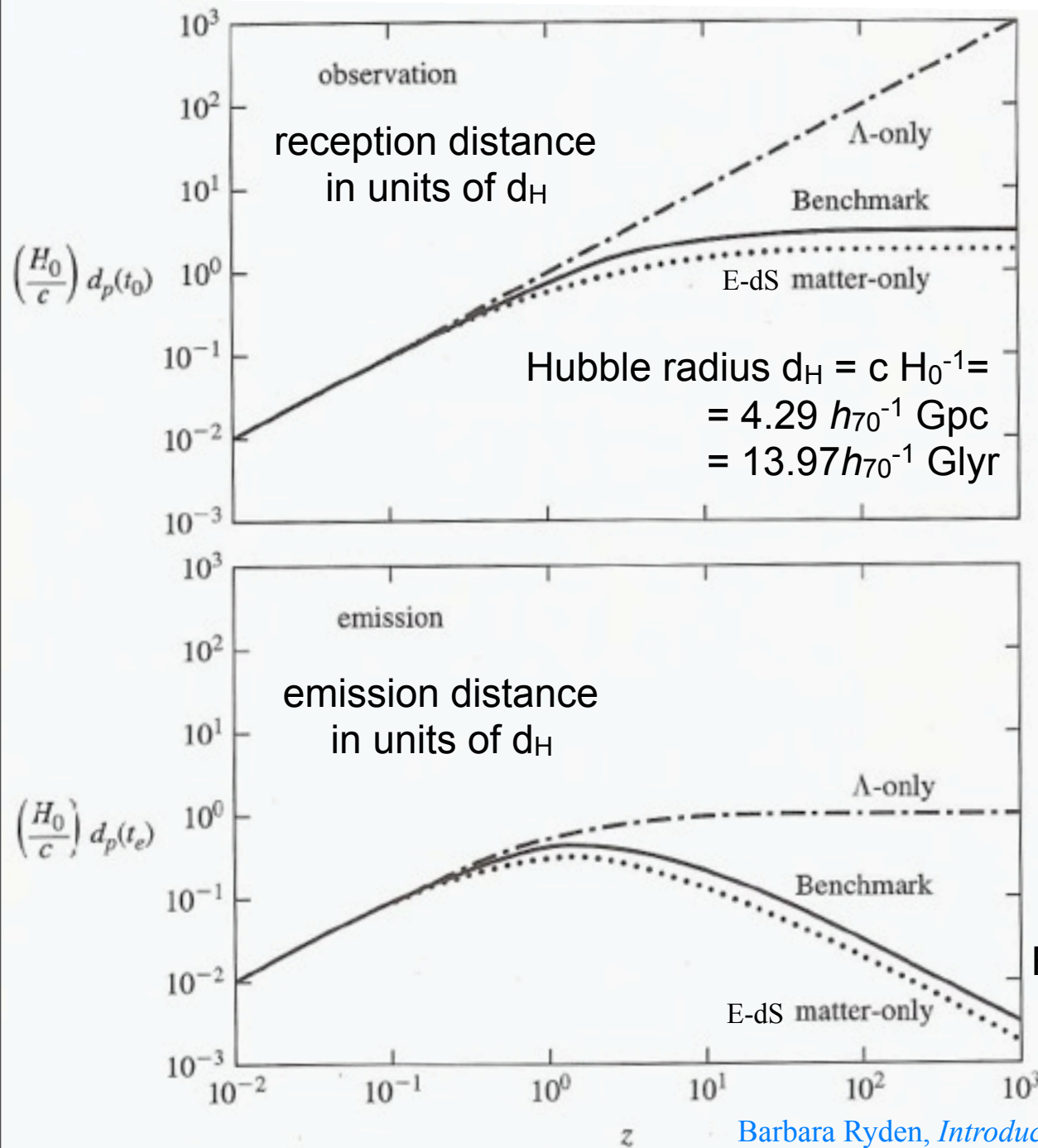
For E-dS, where $H = H_0\,a^{-3/2}$,
$\chi(t_e) = r_e = d_p(t_0) = 2d_H\,(1 - a_e^{1/2})$
$d_p(t_e) = 2d_H\,a_e\,(1 - a_e^{1/2})$

Our Particle Horizon

FRW: $ds^2 = -c^2 dt^2 + a(t)^2 [dr^2 + r^2 d\theta^2 + r^2 \sin^2\theta \, d\phi^2]$ for curvature K=0 so $\sqrt{g_{rr}} = a(t)$

Particle Horizon

d_p(horizon) = (physical distance at time t_0) = $a(t_0) r_p = r_p$

$$d_p\text{(horizon)} = \int_0^{r_{horizon}} dr = r_{horizon} = c\int_0^{t_0} dt/a = c\int_0^1 da/(a^2 H)$$

For E-dS, where $H = H_0 a^{-3/2}$,

$r_{horizon} = \lim_{a_e \to 0} 2d_H (1-a_e^{1/2}) = 2d_H =$

$= 8.58 \, h_{70}^{-1}$ Gpc $= 27.94 \, h_{70}^{-1}$ Glyr

For the Benchmark Model with h=0.70,

$r_{horizon}$ = 13.9 Gpc = 45.2 Glyr.

For the WMAP5 parameters h = 0.70, M = 0.28, K = 0, $r_{horizon}$ = 14.3 Gpc = 46.5 Glyr.

observable universe

Time

now

particle horizon

unobservable universe

Time

O

X

Y

tangent to backward lightcone at big bang

beginning
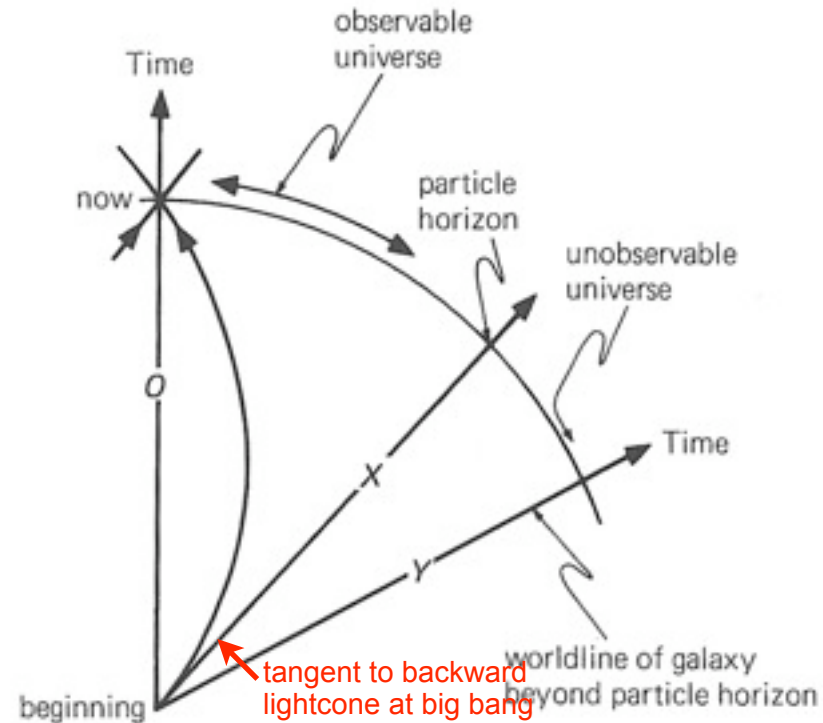
worldline of galaxy beyond particle horizon

Figure 21.11. At the instant labeled "now" the particle horizon is at worldline X. In a big bang universe, all galaxies at the particle horizon have infinite redshift.

Velocities in an Expanding Universe

The velocity away from us now of a galaxy whose light we receive with redshift z_e, corresponding to scale factor $a_e = 1/(1 + z_e)$, is

$$v(t_0) = H_0 \, d_p(t_0)$$

The velocity away from us that this galaxy had when it emitted the light we receive now is
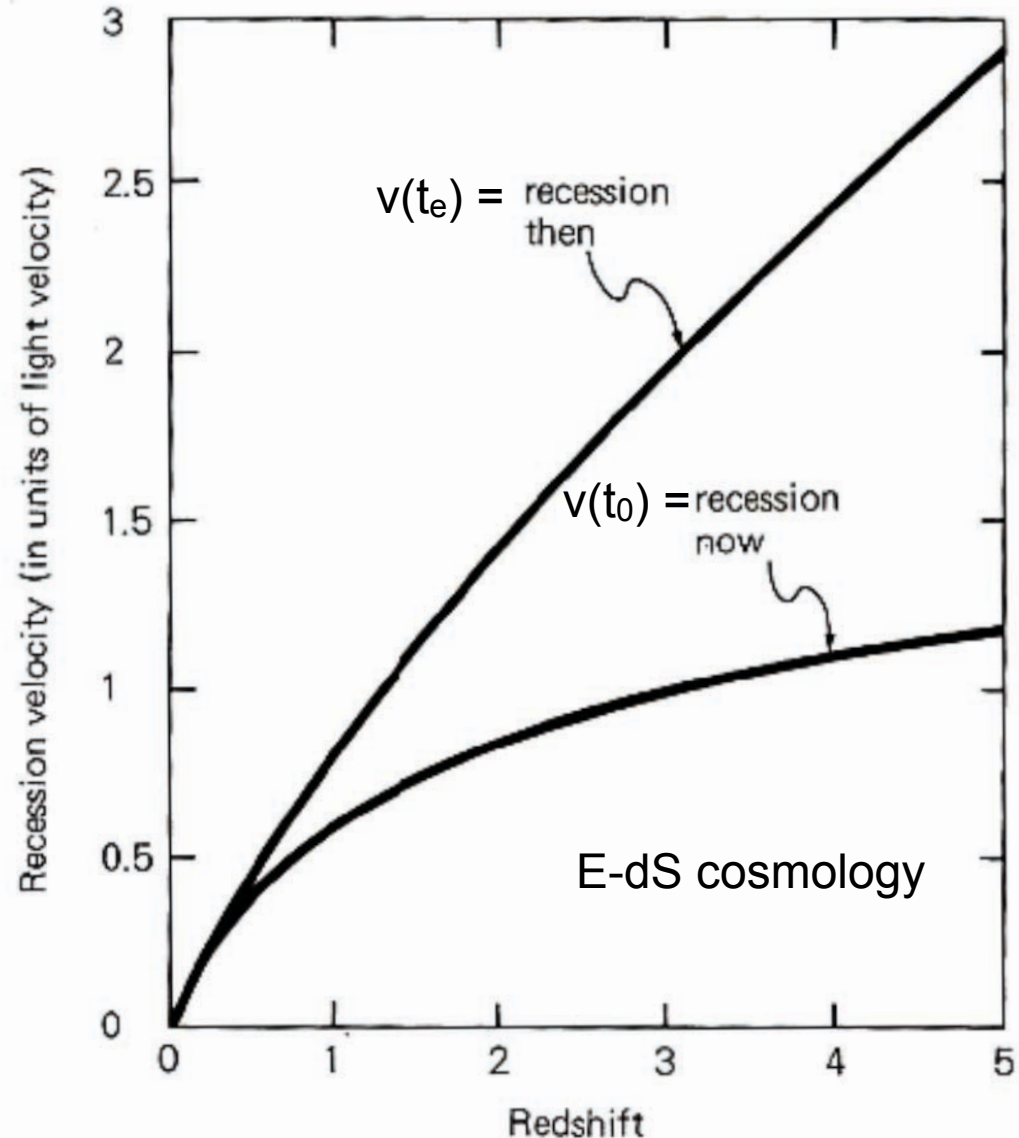
$$v(t_e) = H_e \, d_p(t_e)$$

The graph at right shows $v(t_0)$ and $v(t_e)$ for the E-dS cosmology.
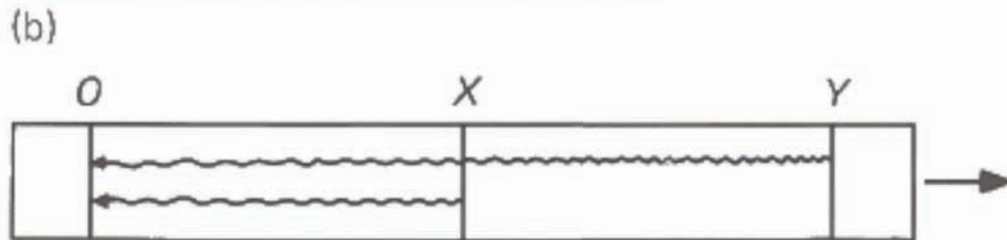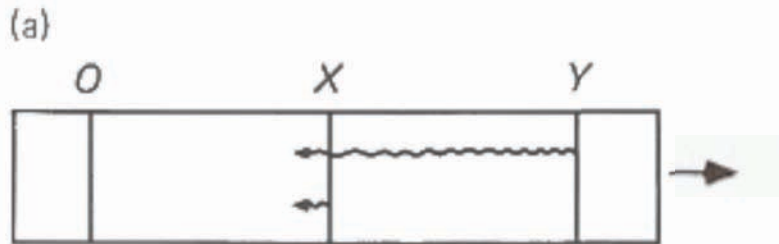
For E-dS, where $H = H_0 \, a^{-3/2}$,

$$v(t_0) = H_0 \, d_p(t_0) = 2c \, (1-a^{1/2})$$

$$v(t_e) = H_e \, d_p(t_e)$$
$$= H_0 \, a_e^{-3/2} \, a_e \, 2c \, (1-a^{1/2})/H_0 = 2c \, (a^{-1/2} - 1)$$

E-dS cosmology

Velocities in an Expanding Universe
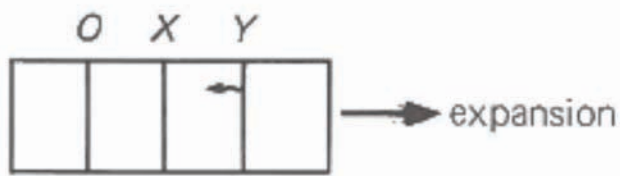
Figure 15.12. On an elastic strip let O represent our position, and X and Y the positions of two galaxies. If signals from X and Y are to reach us at the same instant, then Y, which is farther away, must emit before X. In (a), Y emits a signal. In (b), X emits a signal at a later instant when it is farther away than Y was when it emitted its signal. In (c), both signals arrive simultaneously at O. Y's signal has the greater redshift (it has been stretched more) although Y was closer than X at the time of emission. This odd situation occurs at large redshifts in all big bang universes.
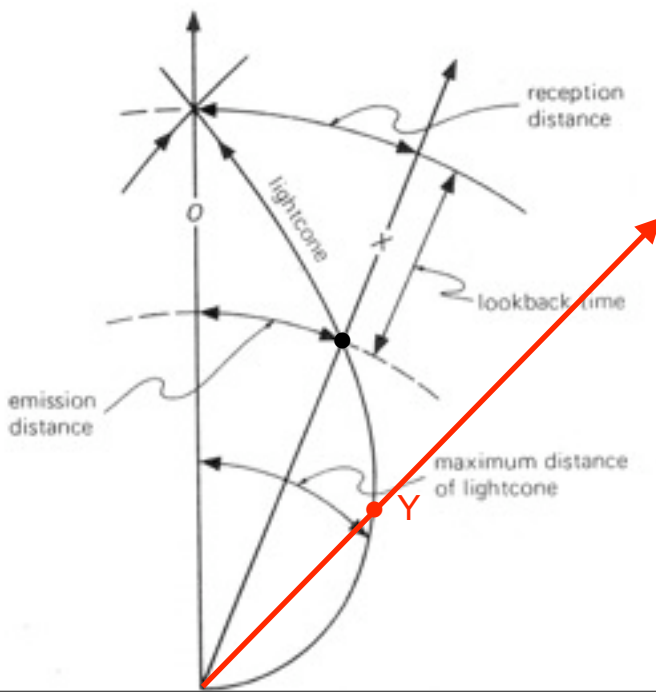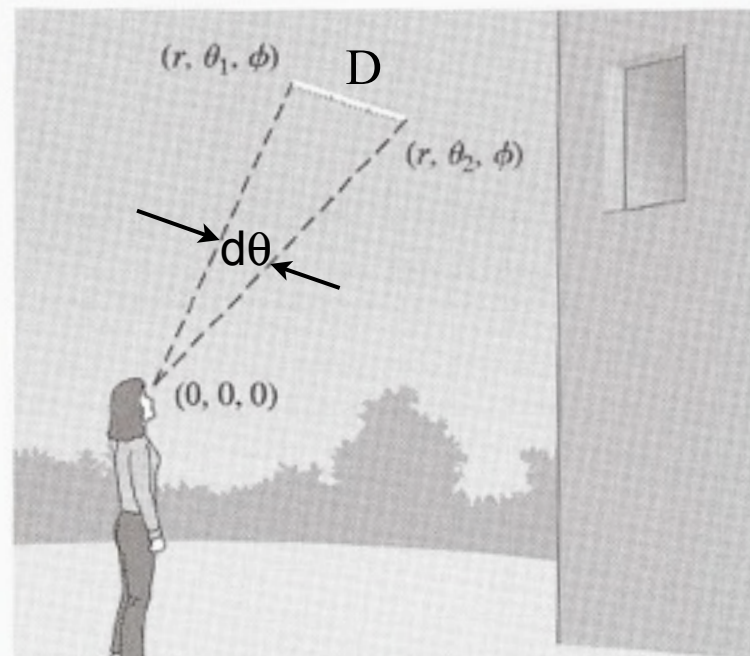
Distances in an Expanding Universe

Angular Diameter Distance

From the FRW metric, the distance D across a source at comoving distance $r = r_e$ which subtends an angle $d\theta = \theta_1 - \theta_2$ is
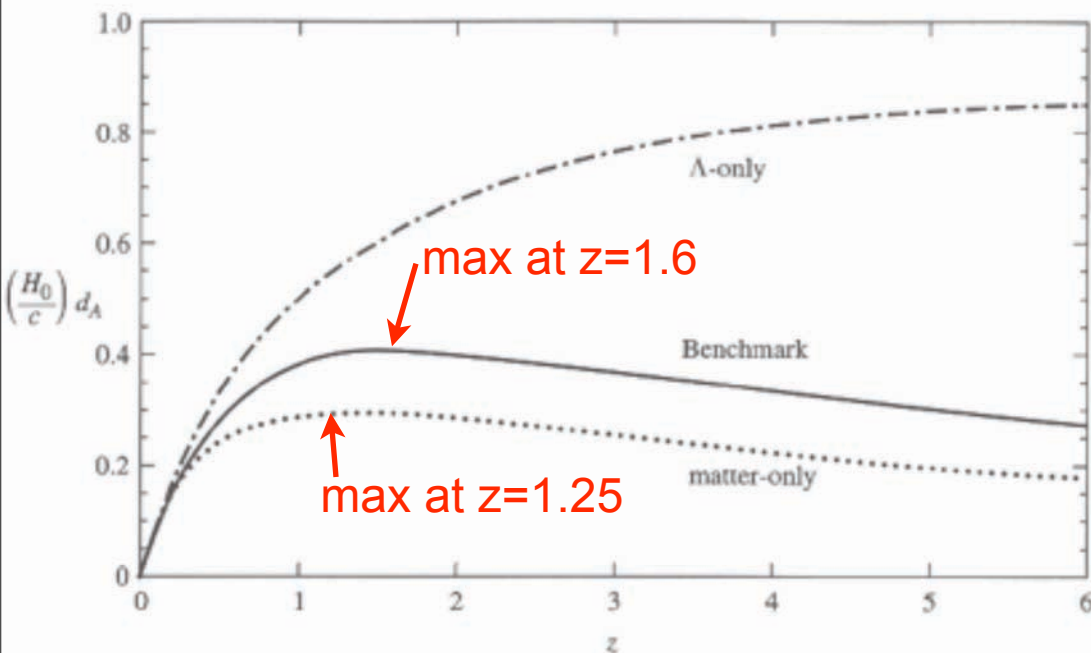
$D = a(t)\, r\, d\theta$, or $d\theta = D/[a(t)\, r]$.

The **angular diameter distance d_A** is defined by $d_A = D/d\theta$, so

$$d_A = a(t_e)\, r_e = r_e/(1+z_e) = d_p(t_e) .$$

This has a maximum, and $d\theta$ a minimum.

Barbara Ryden, *Introduction to Cosmology* (Addison-Wesley, 2003)

max at z=1.6

max at z=1.25

Λ-only

Benchmark

matter-only

For the Benchmark Model

redshift z	D↔1 arcsec
0.1	1.8 kpc
0.2	3.3
0.5	6.1
1	8.0
2	8.4
3	7.7
4	7.0
6	5.7

Distances in an Expanding Universe

In Euclidean space, the **luminosity** L of a source at distance d
is related to the **apparent luminosity** ℓ by ℓ = Power / Area = $L / 4\pi d^2$
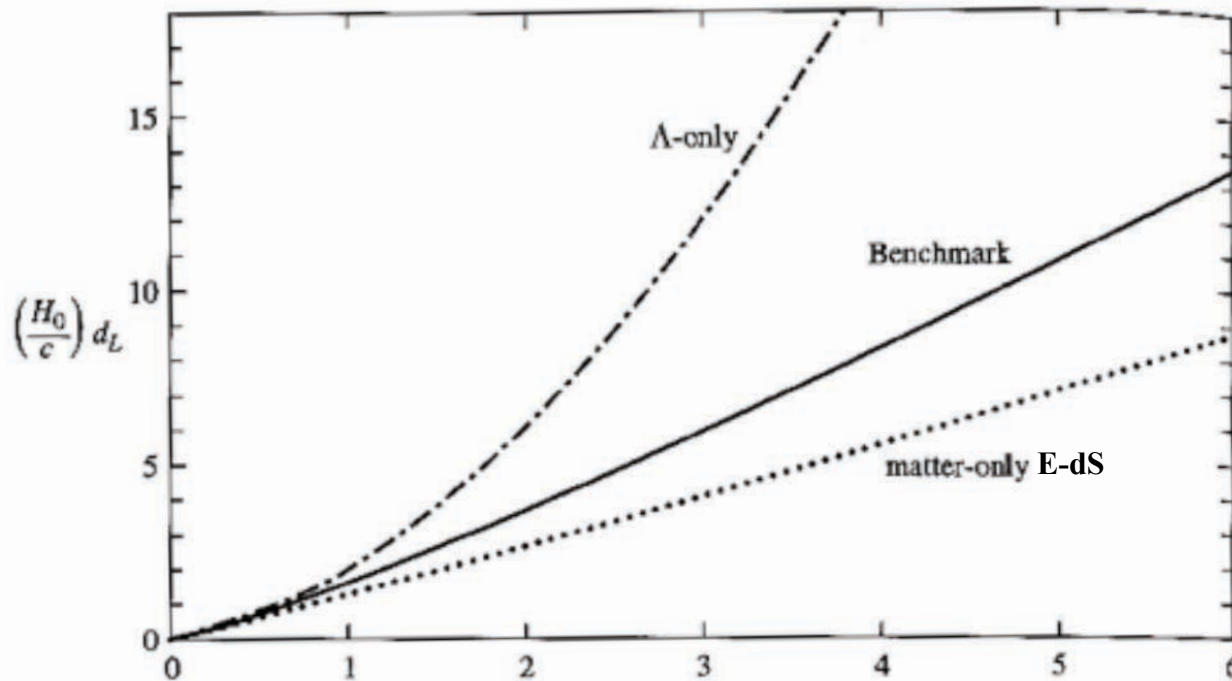The **luminosity distance** d_L is defined by

$$d_L = (L / 4\pi\ell)^{1/2} .$$

Weinberg, *Cosmology*, pp. 31-32, shows that in FRW

$$\ell = \text{Power/Area} = L / 4\pi d_L^2$$

fraction of photons reaching unit area at t_0

$$= L \, [a(t_1)/a(t_0)]^2 / [4\pi d_P(t_0)^2] = L \, a(t_1)^2 / 4\pi r_1^2 = L / 4\pi r_1^2 (1+z_1)^2$$

Thus

(redshift of each photon)(delay in arrival)

$$d_L = r_1/a(t_1) = r_1 (1+z_1) = d_P(t_0) (1+z_1) = d_A (1+z_1)^2$$

Barbara Ryden, *Introduction to Cosmology* (Addison-Wesley, 2003)

redshift $z \rightarrow$

Summary: Distances in an Expanding Universe

FRW: $ds^2 = -c^2 dt^2 + a(t)^2 [dr^2 + r^2 d\theta^2 + r^2 \sin^2\theta \, d\phi^2]$ for curvature K=0 so $\sqrt{g_{rr}} = a(t)$

$\chi(t_1) = $ (comoving distance at time t_1) $= \int_0^{r_1} dr = r_1 = \int_{t_1}^{t_0} dt/a$ adding distances at time t_1

$d(t_1) = $ (physical distance at t_1) $= a(t_1) \chi(t_1) = a_1 r_1$

$\chi(t_1) = $ (comoving distance at time t_0) $= r_1$

$\mathbf{d_p} = $ (physical distance at time t_0) $= a(t_0) r_p = r_p$

since $a(t_0) = 1$

From the FRW metric above, the distance D across a source at comoving distance r_1 which subtends an angle $d\theta$ is $D = a(t_1) r_1 d\theta$. The **angular diameter distance d_A** is defined by $d_A = D/d\theta$, so

$$\mathbf{d_A = a(t_1) \, r_1 = r_1/(1+z_1)}$$

In Euclidean space, the **luminosity** L of a source at distance d is related to the **apparent luminosity** ℓ by

$$\ell = \text{Power/Area} = L/4\pi d^2$$

so the **luminosity distance d_L** is defined by $d_L = (L/4\pi\ell)^{1/2}$.
Weinberg, *Cosmology*, pp. 31-32, shows that in FRW

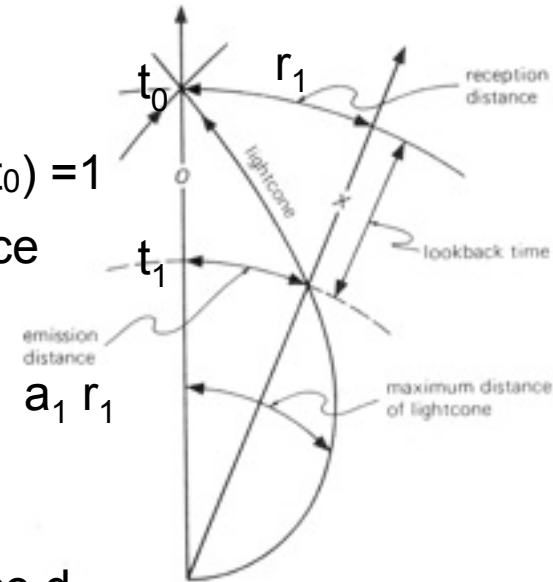$$\ell = \text{Power/Area} = L \, [a(t_1)/a(t_0)]^2 \, [4\pi a(t_0)^2 \, r_1^2]^{-1} = L/4\pi d_L^2$$

fraction of photons reaching unit area at t_0

Thus

$$\mathbf{d_L = r_1/a(t_1) = r_1 \, (1+z_1)}$$

(redshift of each photon)(delay in arrival)

$\chi(t_1) = $ (comoving distance at t

Distances in an Expanding Universe

FRW: $ds^2 = -c^2 dt^2 + a(t)^2 [dr^2 + r^2 d\theta^2 + r^2 \sin^2\theta \, d\phi^2]$ for curvature $k=0$

$=a(t_1)$ for $k=0$

$\chi(t_1) = $ (comoving distance at time t_1) $= \int_0^{r_1} dr \sqrt{g_{rr}} = a(t_1) \, r_1$

$\chi = $ **(comoving distance at time t_0) $= r_1$**   [since $a(t_0)=1$]

From the FRW metric above, the distance D across a source at distance r_1 which subtends an angle $d\theta$ is $D=a(t_1) \, r_1 \, d\theta$. The angular diameter distance d_A is defined by $d_A = D/d\theta$, so

$$d_A = a(t_1) \, r_1 = r_1/(1+z_1)$$

In Euclidean space, the luminosity L of a source at distance d is related to the apparent luminosity ℓ by

$\ell = $ Power/Area $= L/4\pi d^2$

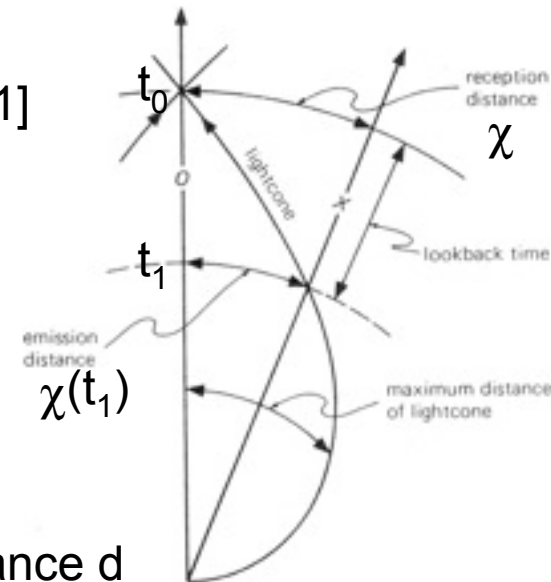so the luminosity distance d_L is defined by $d_L = (L/4\pi\ell)^{1/2}$.

Weinberg, *Gravitation and Cosmology*, pp. 419-421, shows that in FRW

$\ell = $ Power/Area $= L \, [a(t_1)/a(t_0)]^2 \, [4\pi a(t_0)^2 \, r_1^2]^{-1} = L/4\pi d_L^2$

fraction of photons reaching unit area at t_0

Thus

$$d_L = r_1/a(t_1) = r_1 \, (1+z_1)$$

(redshift of each photon)(delay in arrival)

Distances in a Flat (k=0) Expanding Universe

upper curves: Benchmark Model
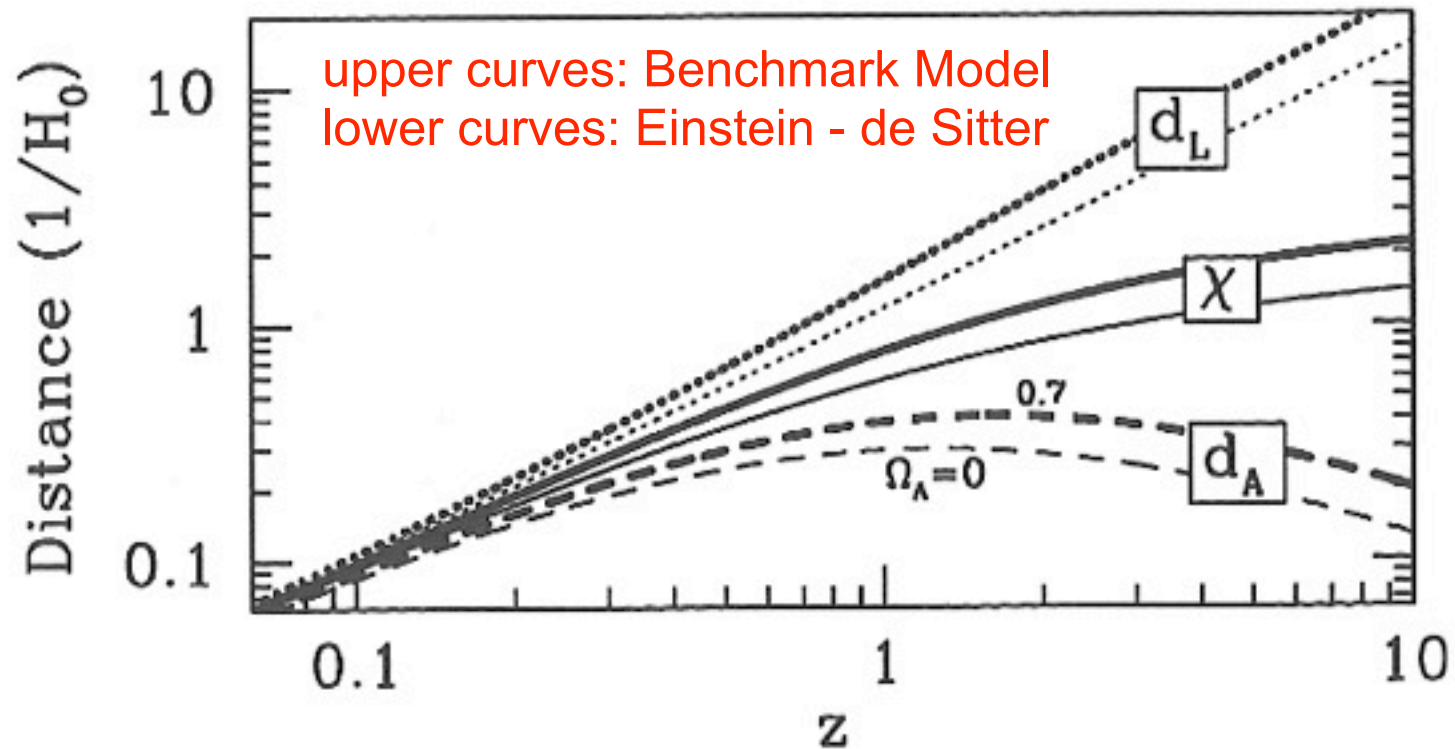lower curves: Einstein - de Sitter

Figure 2.3. Three distance measures in a flat expanding universe. From top to bottom, the luminosity distance, the comoving distance, and the angular diameter distance. The pair of lines in each case is for a flat universe with matter only (light curves) and 70% cosmological constant Λ (heavy curves). In a Λ-dominated universe, distances out to fixed redshift are larger than in a matter-dominated universe.

Distances in the Expanding Universe

D_{now} = proper distance, D_L = luminosity distance,

D_A = angular diameter distance, D_{ltt} = c(t$_0$ − t$_z$)
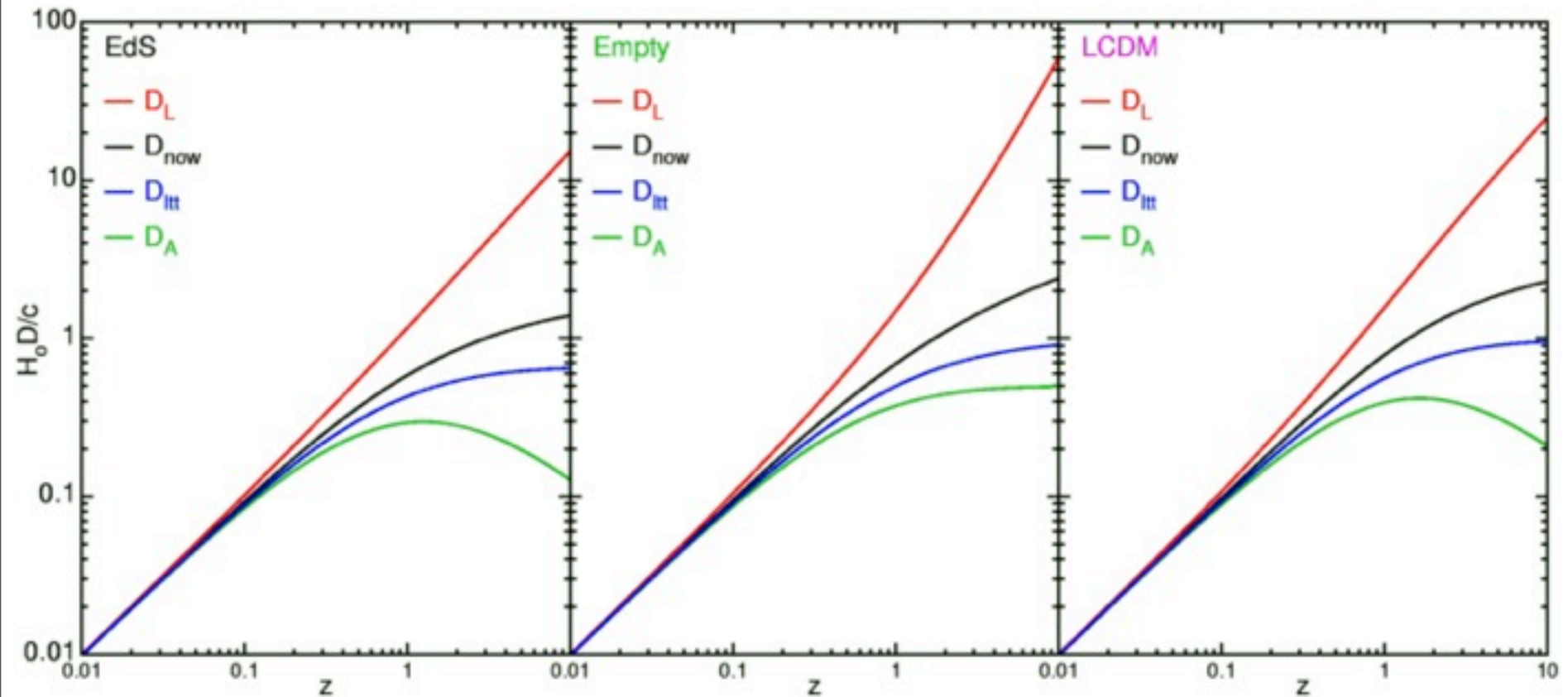
Distances in the Expanding Universe:
Ned Wright's Javascript Calculator

Enter values, hit a button

---

[70] H_o

[0.30] $Omega_M$

[0.83] z

[Open] [Flat]

[0.70] $Omega_{vac}$

[General]

Open sets $Omega_{vac} = 0$ giving an open Universe [if you entered $Omega_M < 1$]

Flat sets $Omega_{vac} = 1 - Omega_M$ giving a flat Universe.

General uses the $Omega_{vac}$ that you entered.

For $\underline{H_o} = 70$, $\underline{Omega_M} = 0.300$, $\underline{Omega_{vac}} = 0.700$, $\underline{z} = 0.830$

- It is now 13.462 Gyr since the Big Bang.
- The age at redshift z was 6.489 Gyr.
- The light travel time was 6.974 Gyr.
- The comoving radial distance, which goes into Hubble's law, is 2868.9 Mpc or 9.357 Gly.
- The comoving volume within redshift z is 98.906 Gpc^3.
- The angular size distance D_A is 1567.7 Mpc or 5.1131 Gly.
- This gives a scale of 7.600 kpc/".
- The luminosity distance D_L is 5250.0 Mpc or 17.123 Gly.

$H_0D_L(z=0.83)$
$=17.123/13.97$
$=1.23$

1 Gly = 1,000,000,000 light years or $9.461*10^{26}$ cm.
1 Gyr = 1,000,000,000 years.
1 Mpc = 1,000,000 parsecs = $3.08568*10^{24}$ cm, or 3,261,566 light years.

Tutorial: Part 1 | Part 2 | Part 3 | Part 4
FAQ | Age | Distances | Bibliography | Relativity

Ned Wright's home page

© 1999-2003 Edward L. Wright. Last modified on 08/13/2003 11:58:51

http://www.astro.ucla.edu/~wright/CosmoCalc.html

See also David W. Hogg, "Distance Measures in Cosmology" http://arxiv.org/abs/astro-ph/9905116

Neutrino Decoupling and Big Bang Nucleosynthesis, Photon Decoupling, and WIMP Annihilation

These will be the next topics covered, although we will probably only be able to start them Wednesday. See Ch. 3 of Dodelson and/or Ch. 3 of Weinberg.

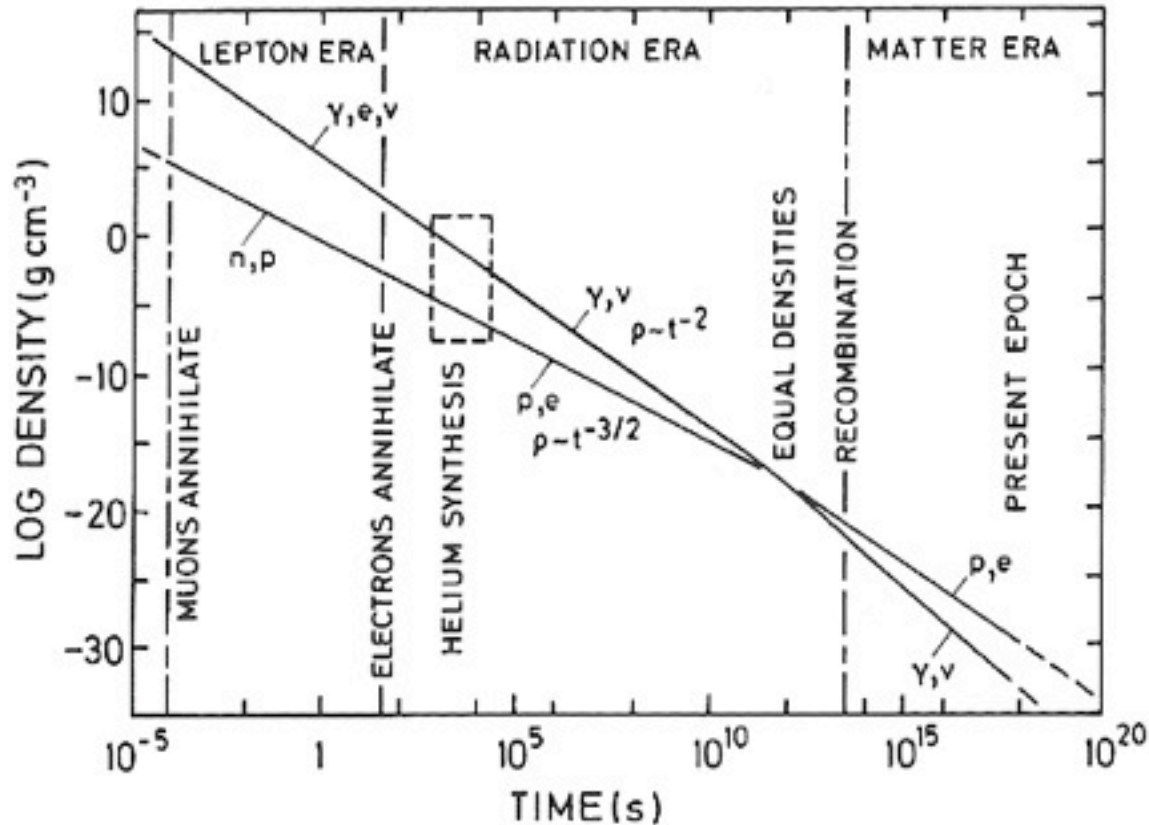# Neutrino Decoupling and Big Bang Nucleosynthesis, Photon Decoupling, and WIMP Annihilation


Fig. 3.1. The thermal history of the standard model. The densities of protons, electrons, photons, and neutrinos are shown at various stages of cosmological evolution [after Harrison (1973)]

Big Bang Nucleosynthesis

BBN was conceived by Gamow in 1946 as an explanation for the formation of all the elements, but the absence of any stable nuclei with A=5,8 makes it impossible for BBN to proceed past Li. The formation of carbon and heavier elements occurs instead through the triple-α process in the centers of red giants (Burbidge[2], Fowler, & Hoyle 57). At the BBN baryon density of $2\times10^{-29}\,\Omega_b\,h^2\,(T/T_0)^3$ g cm^{-3} $\approx 2\times10^{-5}$ g cm^{-3}, the probability of the triple-α process is negligible even though $T \approx 10^9$K.
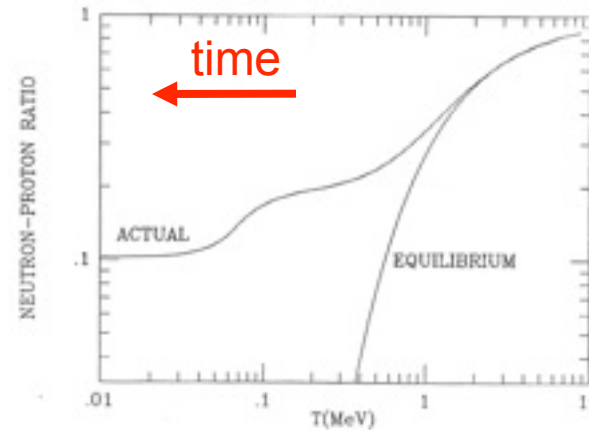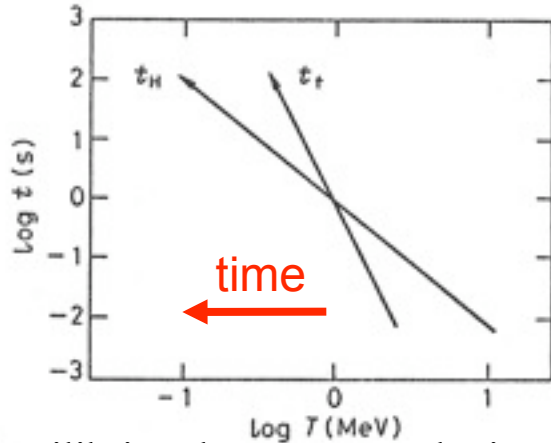
Kolb & Turner

Thermal equilibrium between n and p is maintained by weak interactions, which keeps n/p = exp(-Q/T) (where Q = m_n–m_p = 1.293 MeV) until about $t \approx 1$ s. But because the neutrino mean free time $t_\nu^{-1} \approx \sigma_\nu n_{e\pm} \approx (G_F T)^2 (T^3)$ is increasing as $t_\nu \propto T^{-5}$ (here the Fermi constant $G_F \approx 10^{-5}$ GeV^{-2}), while the horizon size is increasing only as $t_H \approx (G\rho)^{-\frac{1}{2}} \approx M_{Pl}\,T^{-2}$, these interactions freeze out when T drops below about 0.8 MeV. This leaves n/(p+n) ≈ 0.14. The neutrons then decay with a mean lifetime 887 ± 2 s until they are mostly fused into D and then ^{4}He. The higher the baryon density, the higher the final abundance of ^{4}He and the lower the abundance of D that survives this fusion process. Since D/H is so sensitive to baryon density, David Schramm called deuterium the "baryometer." He and his colleagues also pointed out that since the horizon size increases more slowly with T^{-1} the larger the number of light neutrino species N_ν contributing to the energy density ρ, BBN predicted that $N_\nu \approx 3$ before N_ν was measured at accelerators by measuring the width of the Z^0 (Cyburt et al. 2005: $2.67 < N_\nu < 3.85$).

Neutrinos in the Early Universe
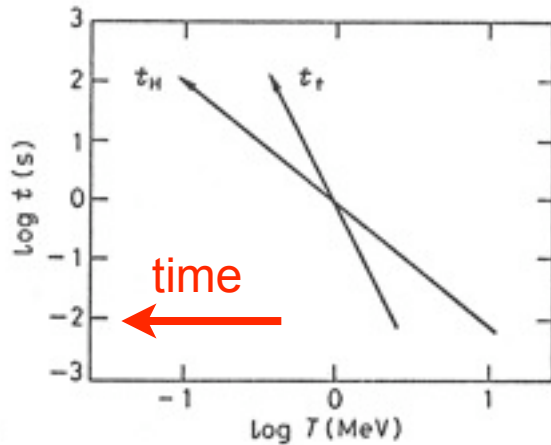
As we discussed, neutrino decoupling occurs at T ~ 1 MeV. After decoupling, the neutrino phase space distribution is

$f_\nu = [1+\exp(p_\nu c/T_\nu)]^{-1}$ (note: $\neq [1+\exp(E_\nu/T_\nu)]$

for NR neutrinos)

After e+e- annihilation, $T_\nu = (4/11)^{1/3} T_\gamma = 1.9$K. Proof :

Number densities of primordial particles

$n_\gamma(T) = 2\,\zeta(3)\,\pi^{-2}\,T^3 = 400$ cm^{-3} $(T/2.7K)^3$, $n_\nu(T) = (3/4)\,n_\gamma(T)$ including antineutrinos

FermiDirac/BoseEinstein factor

Conservation of entropy s_I of interacting particles per comoving volume

$s_I = g_I(T)\,N_\gamma(T) = $ constant, where $N_\gamma = n_\gamma V$; we only include neutrinos for T>1 MeV.

Thus for T>1 MeV, $g_I = 2 + 4(7/8) + 6(7/8) = 43/4$ for γ, e+e-, and the three ν species, while for T< 1 MeV, $g_I = 2 + 4(7/8) = 11/2$. At e+e- annihilation, below about T=0.5 Mev, g_I drops to 2, so that $2N_{\gamma 0} = g_I(T<1$ MeV$)\,N_\gamma(T<1$ MeV$) = (11/2)\,N_\gamma(T<1$ MeV$) = (11/2)(4/3)\,N_\nu(T<1$ MeV$)$. Thus $n_{\nu 0} = (3/4)(4/11)\,n_{\gamma 0} = 109$ cm^{-3} $(T/2.7K)^3$, or

$T_\nu = (4/11)^{1/3}\,T = 0.714\,T$

Statistical Thermodynamics

$$n_i = \frac{g_i}{2\pi^2}\left(\frac{kT_i}{\hbar c}\right)^3 I_i''(\pm), \quad \rho_i = \frac{g_i\, kT_i}{2\pi^2 c^2}\left(\frac{kT_i}{\hbar c}\right)^3 I_i^{21}(\pm), \quad \text{where}$$

$$I_i^{mn} \equiv \int_{\theta_i}^{\infty} x^m \left(x^2 - \theta_i^{-2}\right)^{n/2} \left(e^x \pm 1\right)^{-1} dx, \quad \theta_i = \frac{kT_i}{m_i c^2}, \quad g_i = \text{\# spin states}$$

+ Fermi-Dirac, - Bose-Einstein

$$\theta_i \gg 1 \quad (ER): \quad I''(+) = \tfrac{3}{2}\zeta(3) = 1.803, \quad I^{21}(+) = 7\pi^4/120$$

$$I''(-) = 2\zeta(3) = \boxed{\tfrac{4}{3}} I''(+), \quad I^{21}(-) = \pi^4/15 = \tfrac{8}{7} I^{21}(+)$$

$$\theta_i \ll 1 \quad (NR): \quad n_i = \frac{\rho_i}{m_i} = \frac{g_i}{(2\pi)^{3/2}}\left(\frac{kT_i}{\hbar c}\right)^3 \theta_i^{-3/2} e^{-\theta_i^{-1}} \quad (\text{not } \nu\text{'s})$$

$$\left[\text{Note: } \zeta(3) = 1.2020569\ldots = \sum_{k=1}^{\infty} \frac{1}{k^3} = \prod_{\text{primes}} (1 - p^{-3})^{-1}\right]$$

Boltzmann Equation

$$a^{-3}\frac{d\left(n_1 a^3\right)}{dt} = \int \frac{d^3 p_1}{(2\pi)^3 2E_1} \int \frac{d^3 p_2}{(2\pi)^3 2E_2} \int \frac{d^3 p_3}{(2\pi)^3 2E_3} \int \frac{d^3 p_4}{(2\pi)^3 2E_4}$$

Dodelson (3.1)

$$\times (2\pi)^4 \delta^3(p_1 + p_2 - p_3 - p_4)\delta(E_1 + E_2 - E_3 - E_4)|\mathcal{M}|^2$$

$$\times \{f_3 f_4[1 \pm f_1][1 \pm f_2] - f_1 f_2[1 \pm f_3][1 \pm f_4]\}.$$

+ bosons
- fermions

In the absence of interactions (rhs=0) n_1 falls as a^{-3}

We will typically be interested in T>> E-μ (where μ is the chemical potential). In this limit, the exponential in the Fermi-Dirac or Bose-Einstein distributions is much larger than the ±1 in the denominator, so that

$$f(E) \rightarrow e^{\mu/T} e^{-E/T}$$

and the last line of the Boltzmann equation above simplifies to

$$f_3 f_4[1 \pm f_1][1 \pm f_2] - f_1 f_2[1 \pm f_3][1 \pm f_4]$$

$$\rightarrow \quad e^{-(E_1+E_2)/T}\left\{e^{(\mu_3+\mu_4)/T} - e^{(\mu_1+\mu_2)/T}\right\}.$$

The number densities are given by $\quad n_i = g_i e^{\mu_i/T} \int \frac{d^3 p}{(2\pi)^3} e^{-E_i/T}$. For our applications, i's are

Table 3.1. Reactions in This Chapter: $1 + 2 \leftrightarrow 3 + 4$

	1	2	3	4
Neutron-Proton Ratio	n	ν_e or e^+	p	e^- or $\bar{\nu}_e$
Recombination	e	p	H	γ
Dark Matter Production	X	X	l	l

$$n_i^{(0)} \equiv g_i \int \frac{d^3p}{(2\pi)^3} e^{-E_i/T} = \begin{cases} g_i \left(\frac{m_i T}{2\pi}\right)^{3/2} e^{-m_i/T} & m_i \gg T \\ g_i \frac{T^3}{\pi^2} & m_i \ll T \end{cases} \tag{3.6}$$

With this defintion, $e^{\mu_i/T}$ can be rewritten as $n_i/n_i^{(0)}$, so the last line of Eq. (3.1) is equal to

$$e^{-(E_1+E_2)/T} \left\{ \frac{n_3 n_4}{n_3^{(0)} n_4^{(0)}} - \frac{n_1 n_2}{n_1^{(0)} n_2^{(0)}} \right\}. \tag{3.7}$$

With these approximations the Boltzmann equation now simplifies enormously. Define the thermally averaged cross section as

$$\langle \sigma v \rangle \equiv \frac{1}{n_1^{(0)} n_2^{(0)}} \int \frac{d^3 p_1}{(2\pi)^3 2E_1} \int \frac{d^3 p_2}{(2\pi)^3 2E_2} \int \frac{d^3 p_3}{(2\pi)^3 2E_3} \int \frac{d^3 p_4}{(2\pi)^3 2E_4} e^{-(E_1+E_2)/T}$$

$$\times (2\pi)^4 \delta^3(p_1 + p_2 - p_3 - p_4)\delta(E_1 + E_2 - E_3 - E_4) |\mathcal{M}|^2. \tag{3.8}$$

Then, the Boltzmann equation becomes

$$a^{-3}\frac{d\left(n_1 a^3\right)}{dt} = n_1^{(0)} n_2^{(0)} \langle \sigma v \rangle \left\{ \frac{n_3 n_4}{n_3^{(0)} n_4^{(0)}} - \frac{n_1 n_2}{n_1^{(0)} n_2^{(0)}} \right\}. \tag{3.9}$$

If the reaction rate $n_2\langle\sigma v\rangle$ is much smaller than the expansion rate ($\sim$ H), then the {} on the rhs must vanish. This is called *chemical equilibrium* in the context of the early universe, *nuclear statistical equilibrium* (NSE) in the context of Big Bang nucleosynthesis, and the *Saha equation* when discussing recombination of electrons and protons to form neutral hydrogen.

As the temperature of the universe cools to 1 MeV, the cosmic plasma consists of:

- **Relativistic particles in equilibrium: photons, electrons and positrons.** These are kept in close contact with each other by electromagnetic interactions such as $e^+e^- \leftrightarrow \gamma\gamma$. Besides a small difference due to fermion/boson statistics, these all have the same abundances.

- **Decoupled relativistic particles: neutrinos.** At temperatures a little above 1 MeV, the rate for processes such as $\nu e \leftrightarrow \nu e$ which keep neutrinos coupled to the rest of the plasma drops beneath the expansion rate. Neutrinos therefore share the same temperature as the other relativistic particles, and hence are roughly as abundant, but they do not couple to them.

- **Nonrelativistic particles: baryons.** If there had been no asymmetry in the initial number of baryons and anti-baryons, then both would be completely depleted by 1 MeV. However, such an asymmetry did exist: $(n_b - n_{\bar{b}})/s \sim 10^{-10}$ initially,[1] and this ratio remains constant throughout the expansion. By the time the temperature is of order 1 MeV, all anti-baryons have annihilated away (Exercise 12) so

$$\eta_b \equiv \frac{n_b}{n_\gamma} = 5.5 \times 10^{-10} \left(\frac{\Omega_b h^2}{0.020} \right). \tag{3.11}$$

There are thus many fewer baryons than relativistic particles when $T \sim$ MeV.

Binding Energy per Nucleon

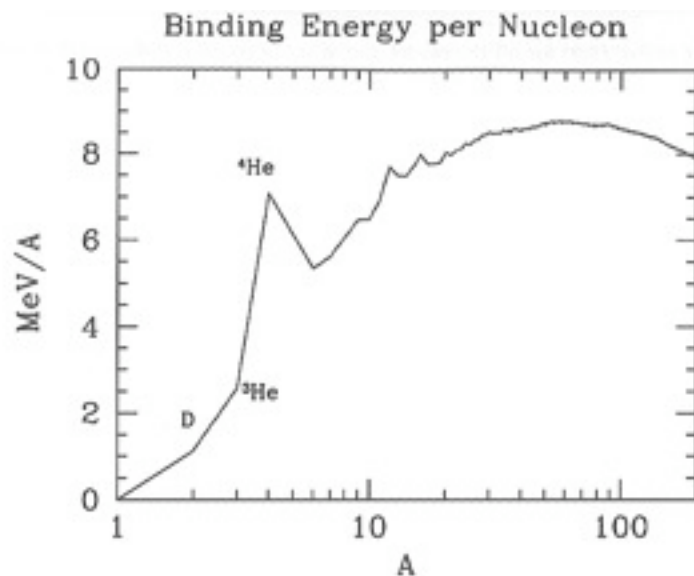**Figure 3.1.** Binding energy of nuclei as a function of mass number. Iron has the highest binding energy, but among the light elements, ^{4}He is a crucial local maximum. Nucleosynthesis in the early universe essentially stops at ^{4}He because of the lack of tightly bound isotopes at $A = 5 - 8$. In the high-density environment of stars, three ^{4}He nuclei fuse to form ^{12}C, but the low baryon number precludes this process in the early universe.

Lightning Introduction to Nuclear Physics

A single proton is a hydrogen nucleus, referred to as ^{1}H or simply p; a proton and a neutron make up deuterium, ^{2}H or D; one proton and two neutrons make tritium, ^{3}H or T. Nuclei with two protons are helium; these can have one neutron (^{3}He) or two (^{4}He). Thus unique elements have a fixed number of protons, and isotopes of a given element have differing numbers of neutrons. The total number of neutrons and protons in the nucleus, the *atomic number*, is a superscript before the name of the element.

The total mass of a nucleus with Z protons and $A - Z$ neutrons differs slightly from the mass of the individual protons and neutrons alone. This difference is called the binding energy, defined as

$$B \equiv Zm_p + (A - Z)m_n - m \tag{3.12}$$

where m is the mass of the nucleus. For example, the mass of deuterium is 1875.62 MeV while the sum of the neutron and proton masses is 1877.84 MeV, so the binding energy of deuterium is 2.22 MeV. Nuclear binding energies are typically in the MeV range, which explains why Big Bang nucleosynthesis occurs at temperatures a bit less than 1 MeV even though nuclear masses are in the GeV range.

Neutrons and protons can interconvert via weak interactions:

$$p + \bar{\nu} \leftrightarrow n + e^+ \quad ; \quad p + e^- \leftrightarrow n + \nu \quad ; \quad n \leftrightarrow p + e^- + \bar{\nu} \tag{3.13}$$

where all the reactions can proceed in either direction. The light elements are built up via electromagnetic interactions. For example, deuterium forms from $p + n \rightarrow D + \gamma$. Then, $D + D \rightarrow n + ^3$He, after which ^{3}He $+ D \rightarrow p + ^4$He produces ^{4}He.

$$\frac{n_D}{n_n n_p} = \frac{n_D^{(0)}}{n_n^{(0)} n_p^{(0)}}. \tag{3.14}$$

The integrals on the right, as given in Eq. (3.6), lead to

$$\frac{n_D}{n_n n_p} = \frac{3}{4} \left(\frac{2\pi m_D}{m_n m_p T} \right)^{3/2} e^{[m_n + m_p - m_D]/T}, \tag{3.15}$$
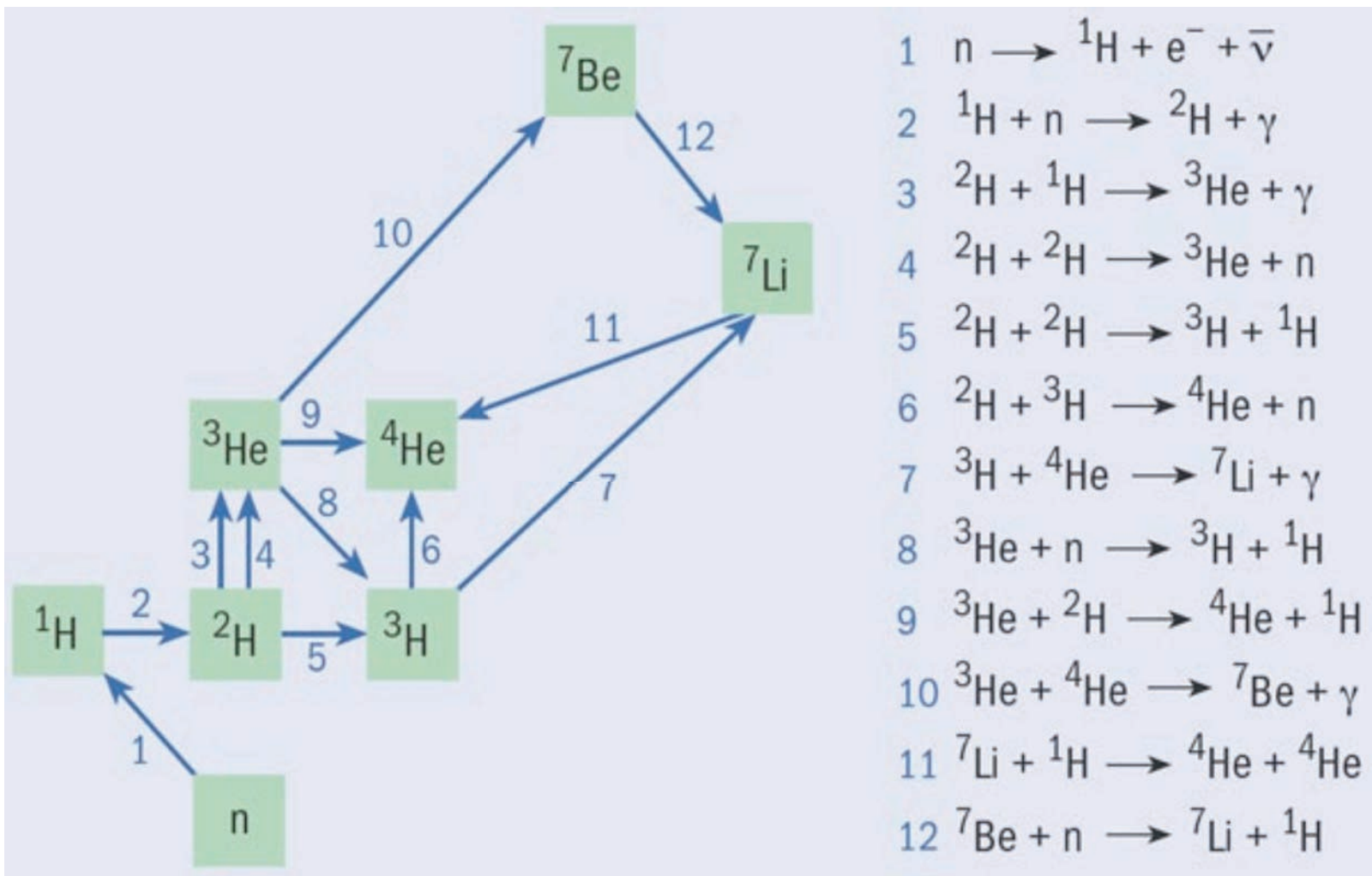
the factor of $3/4$ being due to the number of spin states (3 for D and 2 each for p and n). In the prefactor, m_D can be set to $2m_n = 2m_p$, but in the exponential the small difference between $m_n + m_p$ and m_D is important: indeed the argument of the exponential is by definition equal to the binding energy of deuterium, $B_D = 2.22$ MeV. Therefore, as long as equilibrium holds,

$$\frac{n_D}{n_n n_p} = \frac{3}{4} \left(\frac{4\pi}{m_p T} \right)^{3/2} e^{B_D/T}. \tag{3.16}$$

Both the neutron and proton density are proportional to the baryon density, so roughly,

$$\frac{n_D}{n_b} \sim \eta_b \left(\frac{T}{m_p} \right)^{3/2} e^{B_D/T}. \tag{3.17}$$

$$1 \quad n \longrightarrow {}^{1}H + e^{-} + \bar{\nu}$$

$$2 \quad {}^{1}H + n \longrightarrow {}^{2}H + \gamma$$

$$3 \quad {}^{2}H + {}^{1}H \longrightarrow {}^{3}He + \gamma$$

$$4 \quad {}^{2}H + {}^{2}H \longrightarrow {}^{3}He + n$$

$$5 \quad {}^{2}H + {}^{2}H \longrightarrow {}^{3}H + {}^{1}H$$

$$6 \quad {}^{2}H + {}^{3}H \longrightarrow {}^{4}He + n$$

$$7 \quad {}^{3}H + {}^{4}He \longrightarrow {}^{7}Li + \gamma$$

$$8 \quad {}^{3}He + n \longrightarrow {}^{3}H + {}^{1}H$$

$$9 \quad {}^{3}He + {}^{2}H \longrightarrow {}^{4}He + {}^{1}H$$

$$10 \quad {}^{3}He + {}^{4}He \longrightarrow {}^{7}Be + \gamma$$

$$11 \quad {}^{7}Li + {}^{1}H \longrightarrow {}^{4}He + {}^{4}He$$

$$12 \quad {}^{7}Be + n \longrightarrow {}^{7}Li + {}^{1}H$$

Deuterium nuclei (^{2}H) were produced by collisions between protons and neutrons, and further nuclear collisions led to every neutron grabbing a proton to form the most tightly bound type of light nucleus: ^{4}He. This process was complete after about five minutes, when the universe became too cold for nuclear reactions to continue. Tiny amounts of deuterium, ^{3}He, ^{7}Li, and ^{7}Be were produced as by-products, with the ^{7}Be undergoing beta decay to form ^{7}Li. Almost all of the protons that were not incorporated into ^{4}He nuclei remained as free particles, and this is why the universe is close to 25% ^{4}He and 75% H by mass. The other nuclei are less abundant by several orders of magnitude.
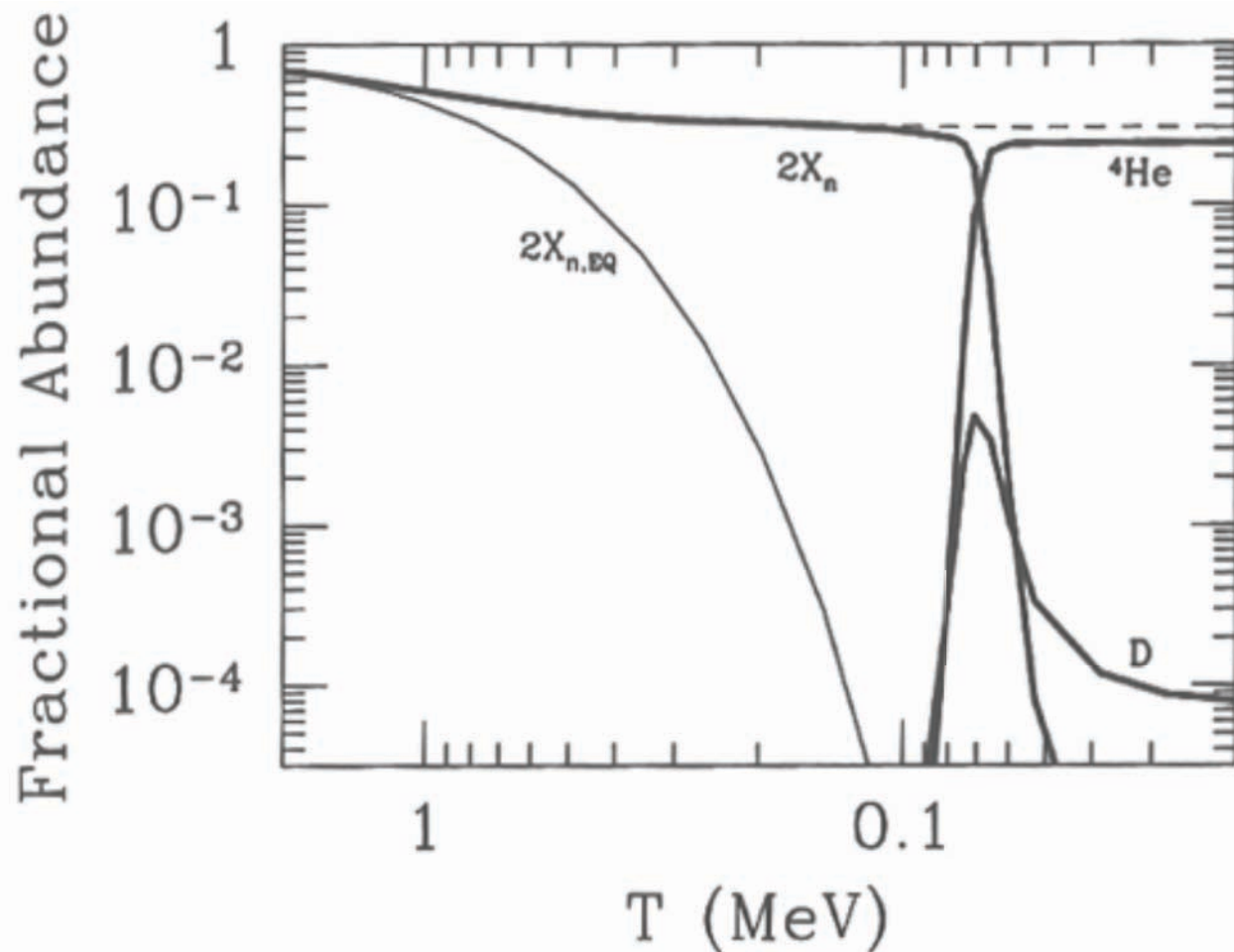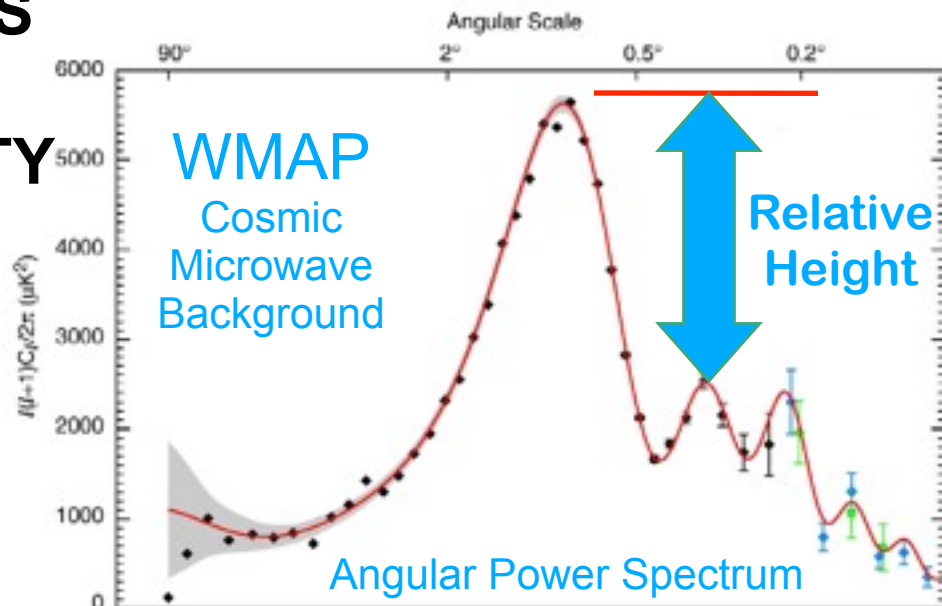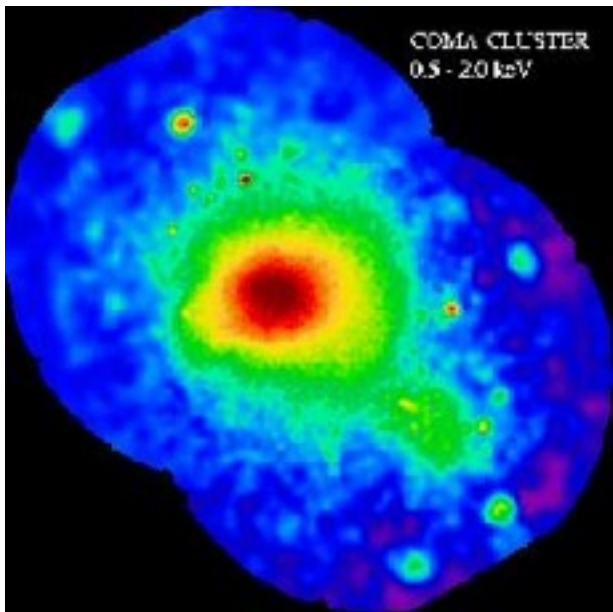
Figure 3.2. Evolution of light element abundances in the early universe. Heavy solid curves are results from Wagoner (1973) code; dashed curve is from integration of Eq. (3.27); light solid curve is twice the neutron equilibrium abundance. Note the good agreement of Eq. (3.27) and the exact result until the onset of neutron decay. Also note that the neutron abundance falls out of equilibrium at $T \sim$ MeV.
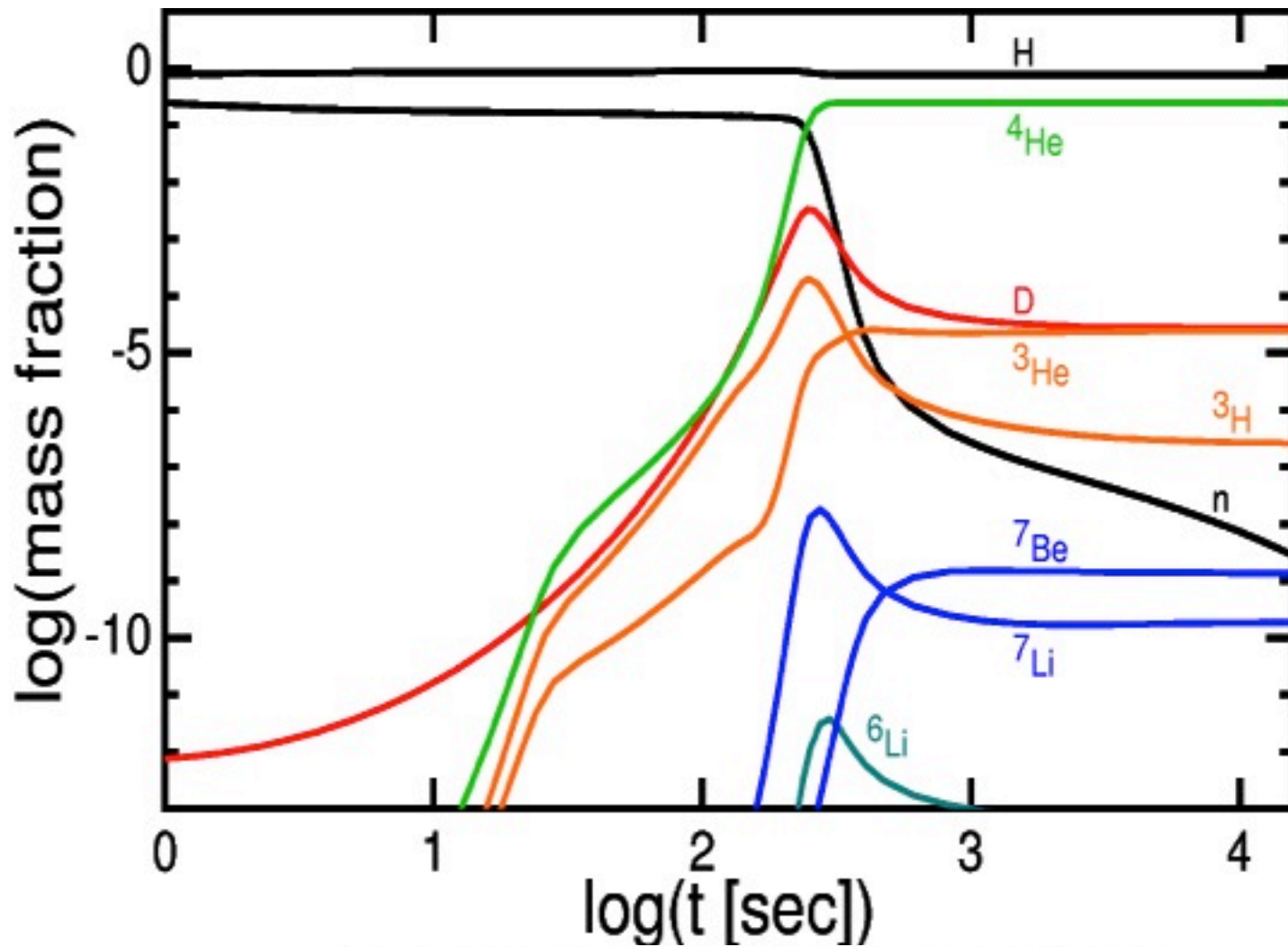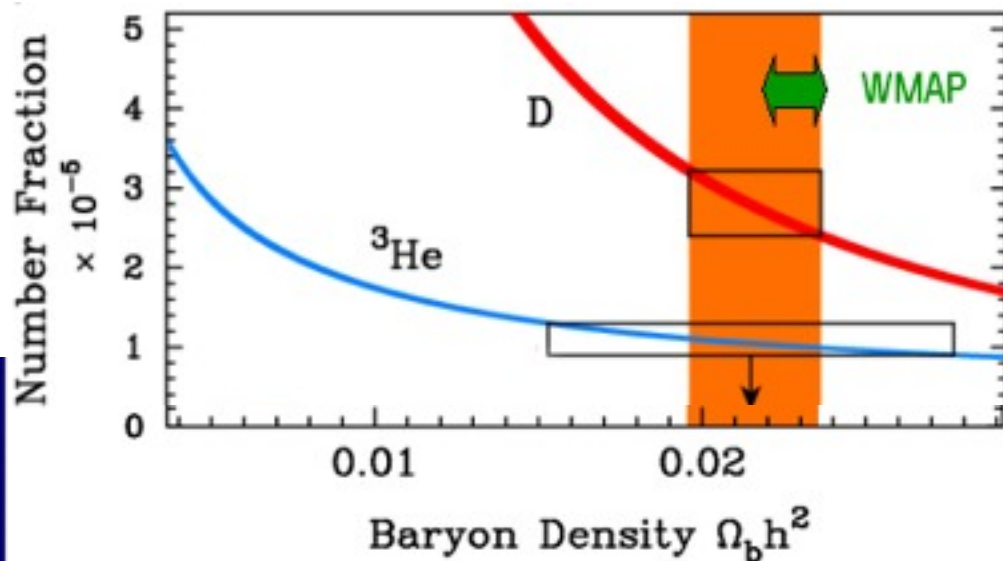
The detailed production of the lightest elements out of protons and neutrons during the first three minutes of the universe's history. The nuclear reactions occur rapidly when the temperature falls below a billion degrees Kelvin. Subsequently, the reactions are shut down, because of the rapidly falling temperature and density of matter in the expanding universe.

Ken Kawano's (1992) BBN code is available at
http://www-thphys.physics.ox.ac.uk/users/SubirSarkar/bbn.html

5 INDEPENDENT MEASURES AGREE: ATOMS ARE ONLY 4% OF THE COSMIC DENSITY

Galaxy Cluster in X-rays

COMA CLUSTER
0.5 - 2.0 keV

WMAP
Cosmic Microwave Background

Relative Height

Angular Power Spectrum

Deuterium Abundance + Big Bang Nucleosynthesis

Absorption of Quasar Light

Q1422+2309 z=3.62

& WIGGLES IN GALAXY P(k)

Periodic Table

White - Big Bang
Yellow - Small Stars
Blue - Supernovae
Pink - Cosmic Rays
Green - Large Stars

VISIBLE MATTER

ALL OTHER VISIBLE ATOMS
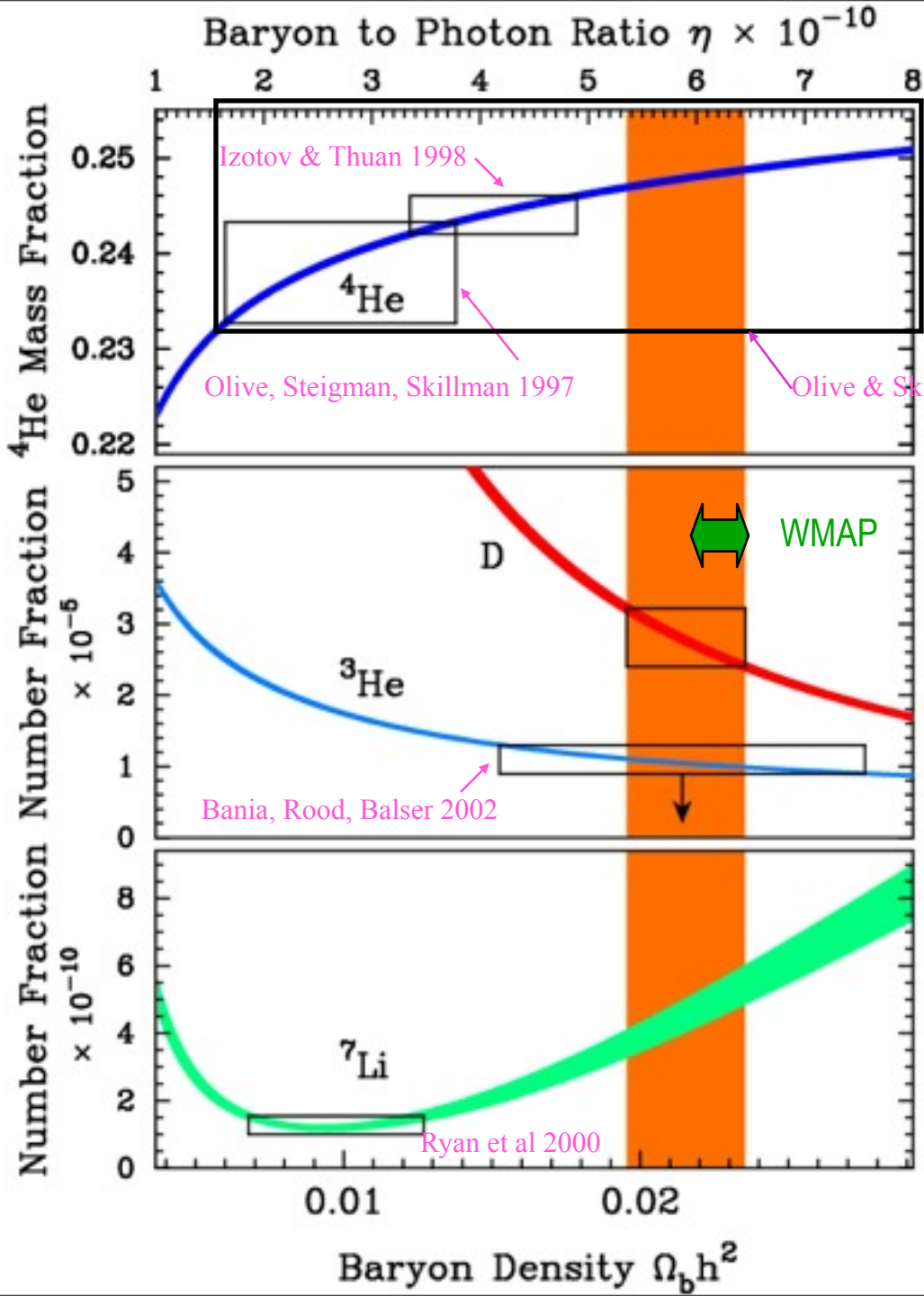
HYDROGEN AND HELIUM

NOVUS ORDO SECLORUM

stardust

stars

COSMIC DENSITY PYRAMID
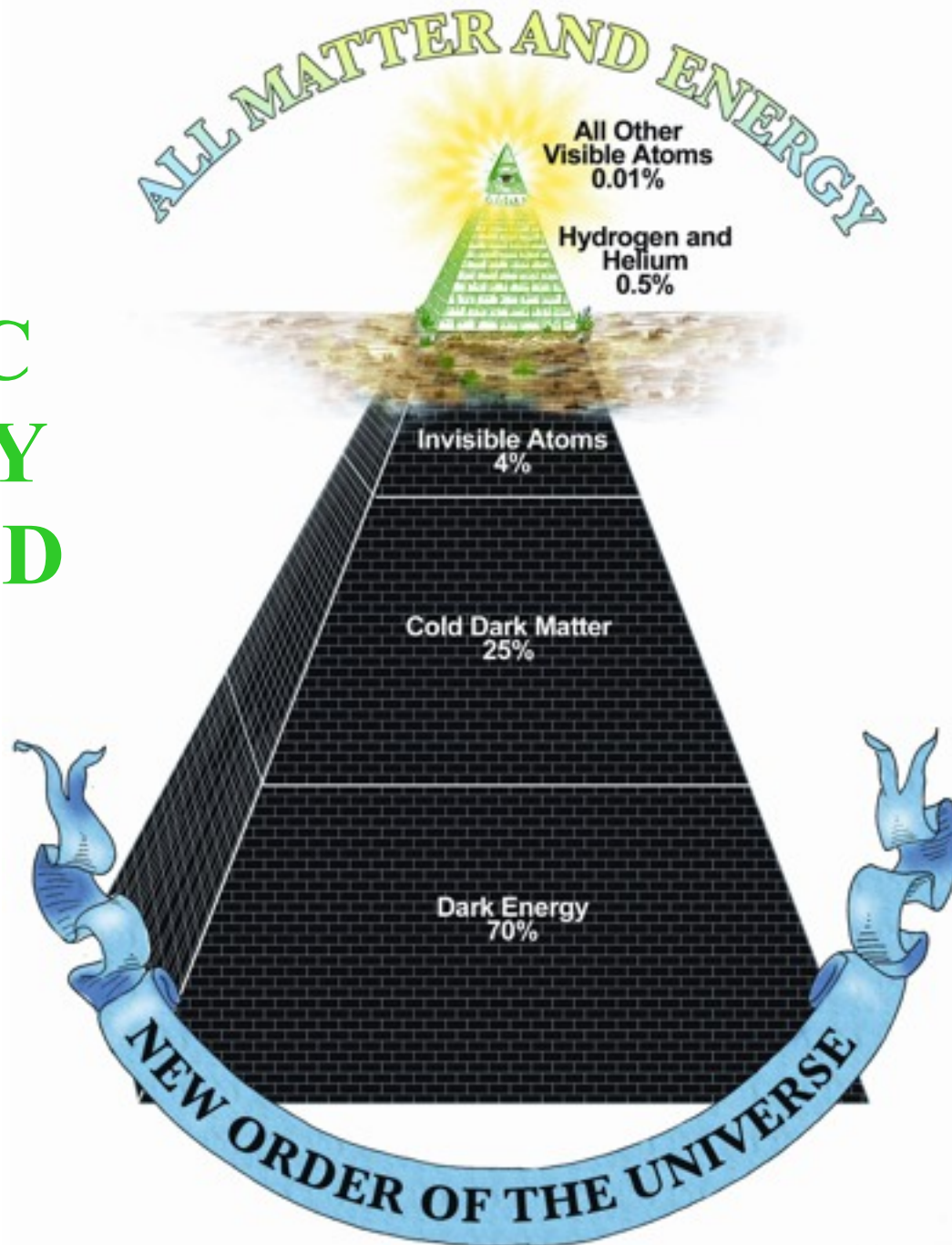
BBN Predicted vs. Measured Abundances of D, ^{3}He, ^{4}He, and ^{7}Li

^{7}Li IS NOW DISCORDANT unless stellar diffusion destroys ^{7}Li

Baryon to Photon Ratio $\eta \times 10^{-10}$

Izotov & Thuan 1998

Izotov & Thuan 2004: $\Omega_b h^2 = 0.012 \pm 0.0025$

^{4}He Mass Fraction

^{4}He

Olive, Steigman, Skillman 1997

Olive & Skillman 2004: **big uncertainties**

$\times 10^{-5}$ Number Fraction

D

WMAP

WMAP (Spergel et al. 2003) says that $\Omega_b h^2 = 0.0224 \pm 0.0009$ (with their running spectral index model)

^{3}He

Bania, Rood, Balser 2002

BBN predictions are from Burles, Nollett, & Turner 2001

Number Fraction $\times 10^{-10}$

^{7}Li

Ryan et al 2000

D/H is from Kirkman, Tytler, Suzuki, O'Meara, & Lubin 2004, giving $\Omega_b h^2 = 0.0214 \pm 0.0020$

Baryon Density $\Omega_b h^2$

Deuterium absorption at redshift 2.525659 towards Q1243+3047
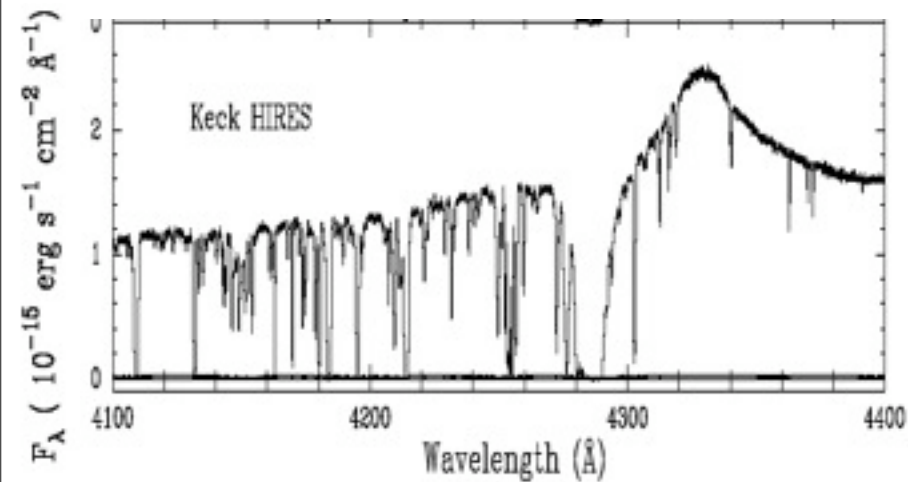
The Lyα absorption near 4285 Å is from the system in which we measure D/H.

The detection of Deuterium and the modeling of this system seem convincing. This is just a portion of the evidence that the Tytler group presented in this paper. They have similarly convincing evidence for several other Lyman alpha clouds in quasar spectra.
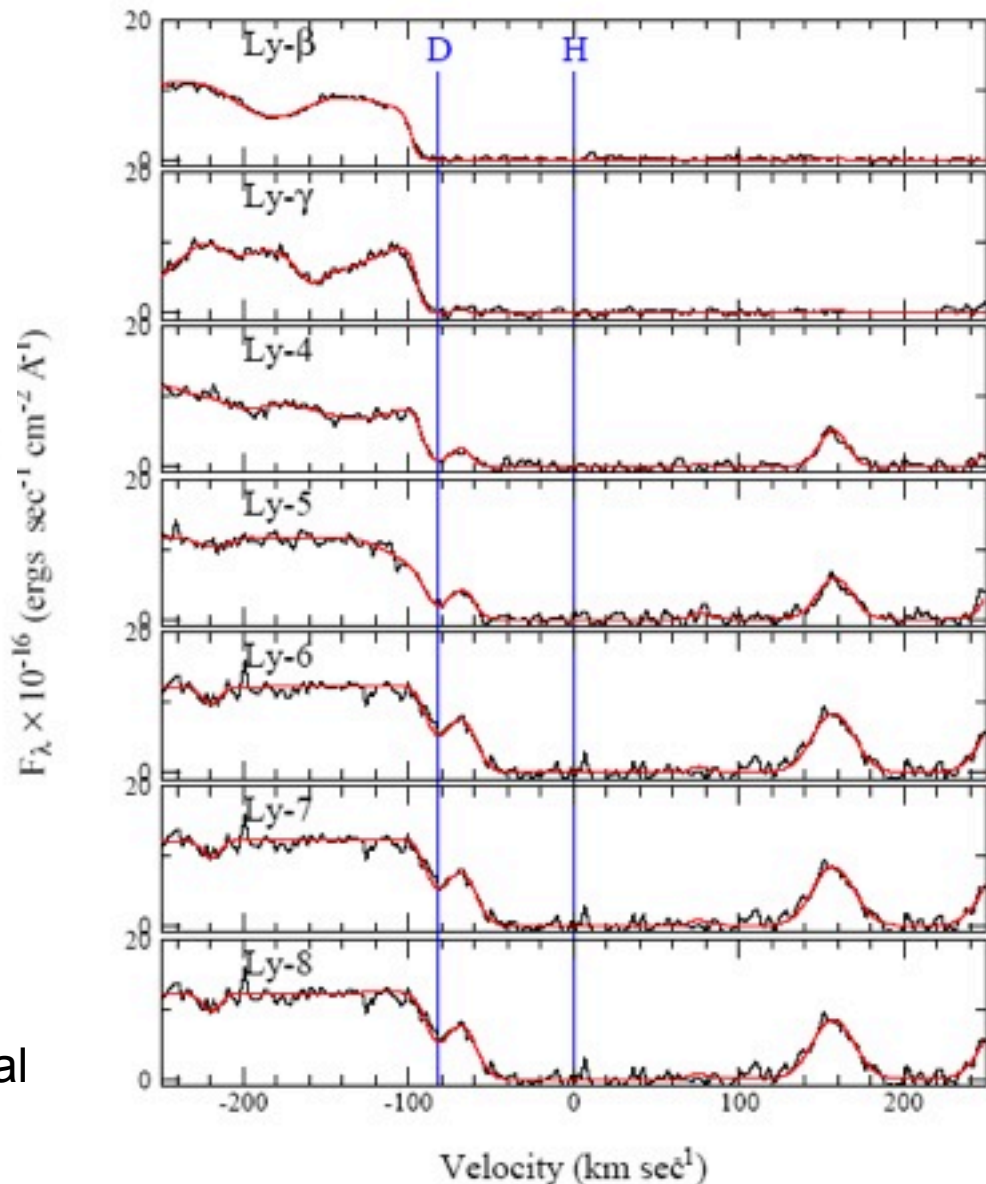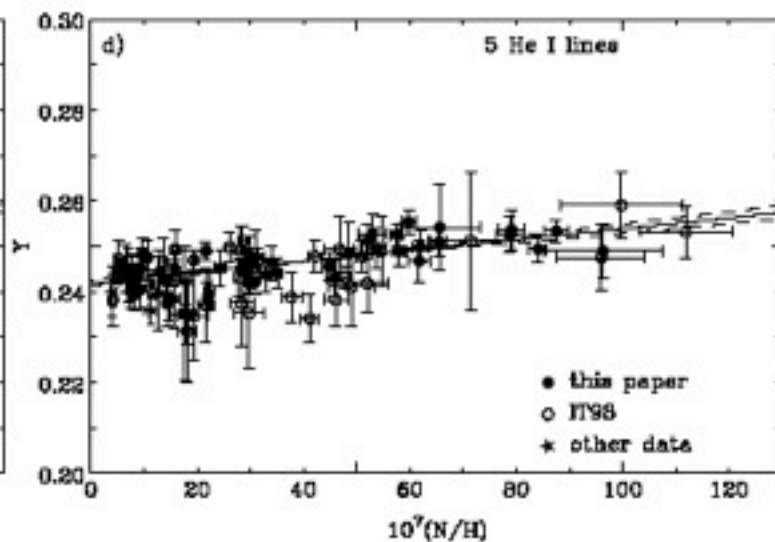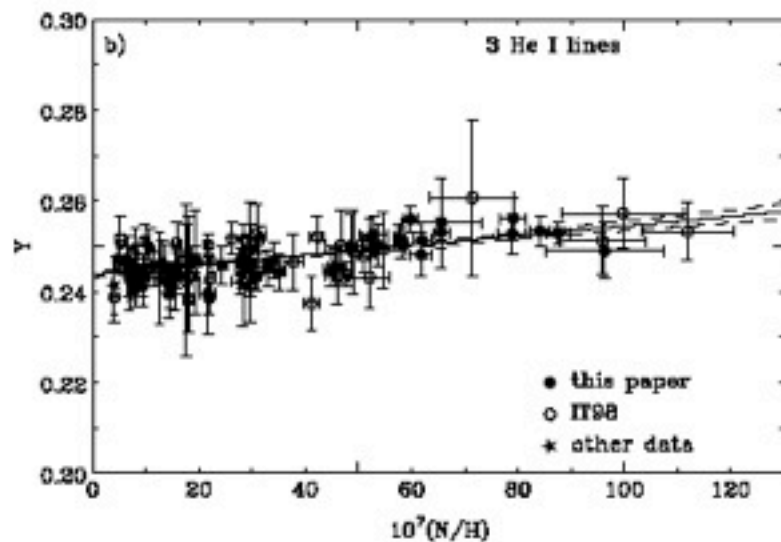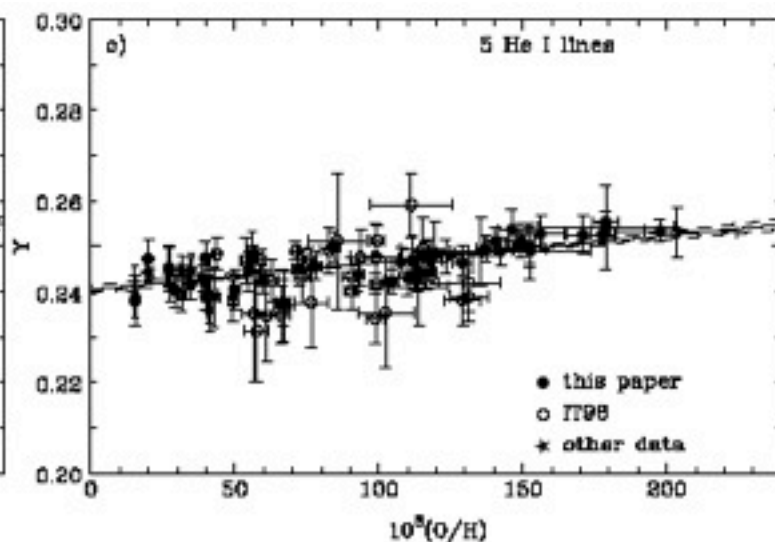

FIG. 7.— The HIRES spectrum of Ly-2 to 8, together with our model of the system, as given in Table 3.

Kirkman, Tytler, Suzuki, O'Meara, & Lubin 2004

Determination of primordial He⁴ abundance Y_p by linear regression
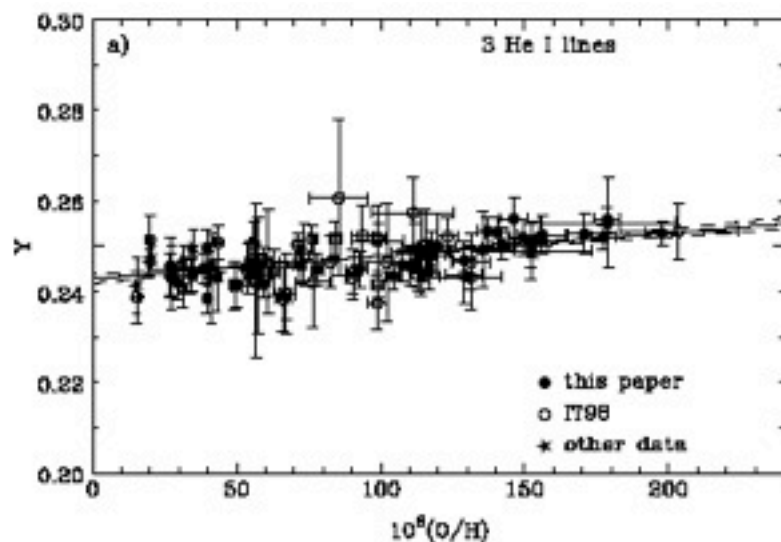
$Y = M(^4He)/M(baryons)$, Primordial $Y \equiv Y_p$ = zero intercept

Note: BBN plus D/H $\Rightarrow Y_p = 0.247 \pm 0.001$

Izotov & Thuan 2004

The Li abundance disagreement with BBN may indicate new physics

Did Something Decay, Evaporate, or Annihilate during Big Bang Nucleosynthesis?

Karsten Jedamzik   Phys.Rev. D70 (2004) 063524

Laboratoire de Physique Mathématique et Théorique, C.N.R.S.,
Université de Montpellier II, 34095 Montpellier Cedex 5, France

Results of a detailed examination of the cascade nucleosynthesis resulting from the putative hadronic decay, evaporation, or annihilation of a primordial relic during the Big Bang nucleosynthesis (BBN) era are presented. It is found that injection of energetic nucleons around cosmic time 10^3sec may lead to an observationally favored reduction of the primordial ^{7}Li/H yield by a factor $2-3$. Moreover, such sources also generically predict the production of the ^{6}Li isotope with magnitude close to the as yet unexplained high ^{6}Li abundances in low-metallicity stars. The simplest of these models operate at fractional contribution to the baryon density $\Omega_b h^2 \gtrsim 0.025$, slightly larger than that inferred from standard BBN. Though further study is required, such sources, as for example due to the decay of the next-to-lightest supersymmetric particle into GeV gravitinos or the decay of an unstable gravitino in the TeV range of abundance $\Omega_C h^2 \sim 5 \times 10^{-4}$ show promise to explain both the ^{6}Li and ^{7}Li abundances in low metallicity stars.

See also "Supergravity with a Gravitino LSP" by Jonathan L. Feng, Shufang Su, Fumihiro Takayama Phys.Rev. D70 (2004) 075019

"Gravitino Dark Matter and the Cosmic Lithium Abundances" by Sean Bailly, Karsten Jedamzik, Gilbert Moultaka, arXiv:0812.0788

# The Li abundance disagreement with BBN may be caused by stellar diffusion
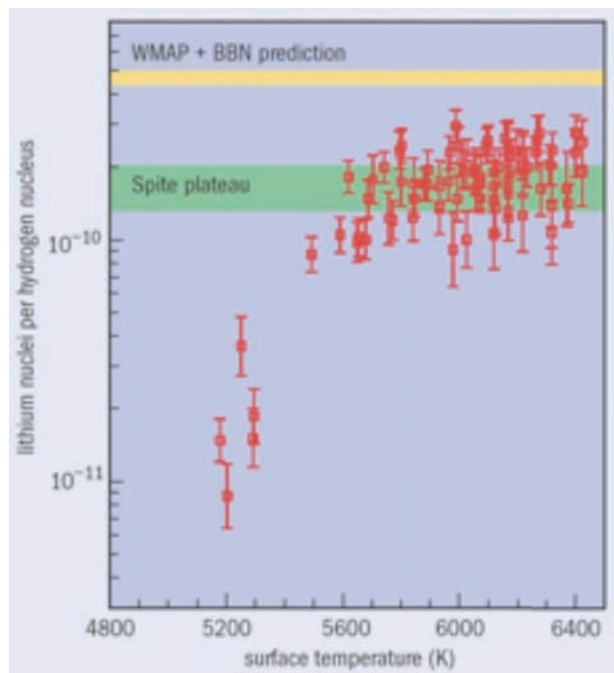
Lithium abundance in very old stars that formed from nearly primordial gas. The amount of ^{7}Li in these "Spite-plateau" stars (green) is much less than has been inferred by combining BBN with measurements of the cosmic microwave background made using WMAP (yellow band). Our understanding of stellar astrophysics may be at fault. Those Spite-plateau stars that have surface temperatures between 5700 and 6400 K have uniform abundances of ^{7}Li because the shallow convective envelopes of these warm stars do not penetrate to depths where the temperature exceeds that for ^{7}Li to be destroyed ($T_{destruct} = 2.5 \times 10^6$ K). The envelopes of cooler stars (data points towards the left of the graph) do extend to such depths, so their surfaces have lost ^{7}Li to nuclear reactions. **If the warm stars gradually circulate ^{7}Li from the convective envelope to depths where $T > T_{destruct}$, then their surfaces may also slowly lose their ^{7}Li.** From http://physicsworld.com/cws/article/print/30680
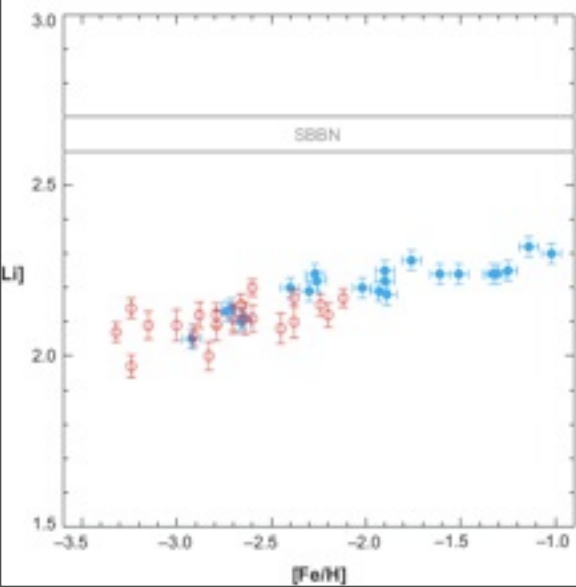
Lithium abundances, [Li] $\equiv$ 12+ log(Li/H), versus metallicity (on a log scale relative to solar) from (red) S. Ryan et al. 2000, ApJ, 530, L57; (blue) M. Asplund et al.2006, ApJ, 644, 229. Figure from G. Steigman 2007, ARAA 57, 463.

Korn et al. 2006 find that both lithium and iron have settled out of the atmospheres of these old stars, and they infer for the unevolved abundances, [Fe/H] = −2.1 and [Li] = 2.54 ± 0.10, in excellent agreement with SBBN.

The most stringent constraint on a mixing model is that it must maintain the observed tight bunching of plateau stars that have the same average ^{7}Li abundance. In a series of papers that was published between 2002 and 2004, Olivier Richard and collaborators at the Université de Montréal in Canada proposed such a mixing model that has since gained observational support. It suggests that all nuclei heavier than hydrogen settle very slowly out of the convective envelope under the action of gravity. In particular, the model makes specific predictions for settling as a star evolves, which are revealed as variations of surface composition as a function of mass in stars that formed at the same time.
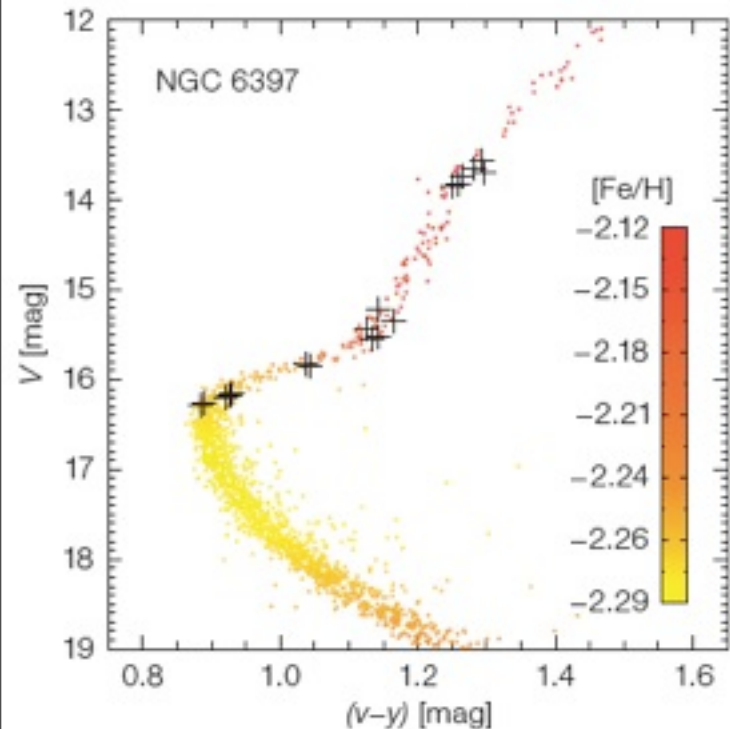
NGC 6397

By spring 2006, Andreas Korn of Uppsala University in Sweden and colleagues had used the European Southern Observatory's Very Large Telescope (VLT) in Chile to study 18 chemically primitive stars in a distant globular cluster called NGC 6397 that were known to have the same age and initial composition. From this Korn et al. showed that the iron and lithium abundances in these stars both varied according to stellar mass as predicted by Richard's model. In fact, the model indicated that the observed stars started out with a ^{7}Li abundance that agrees with the WMAP data. Corroboration of these results is vital because **if the result stands up to scrutiny based on a wide range of data, then we have solved the lithium problem.**

Korn et al. The Messenger 125 (Sept 2006);
Korn et al. 2006, Nature 442, 657.

A probable stellar solution to the cosmological lithium discrepancy
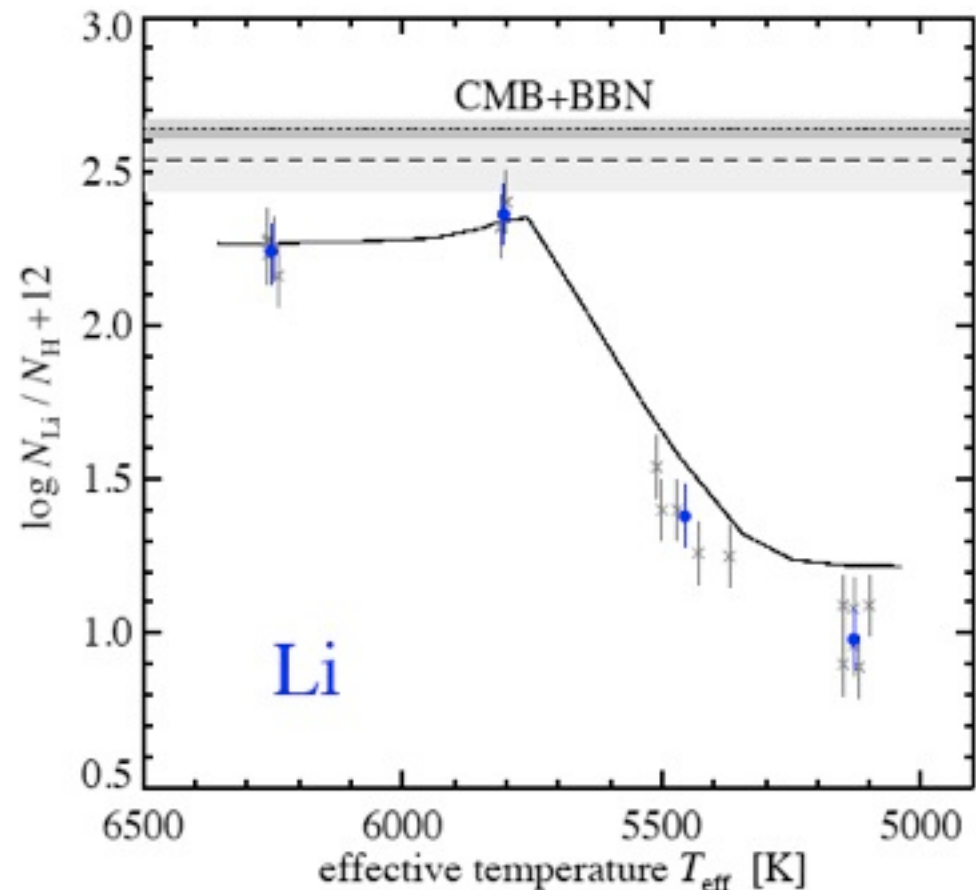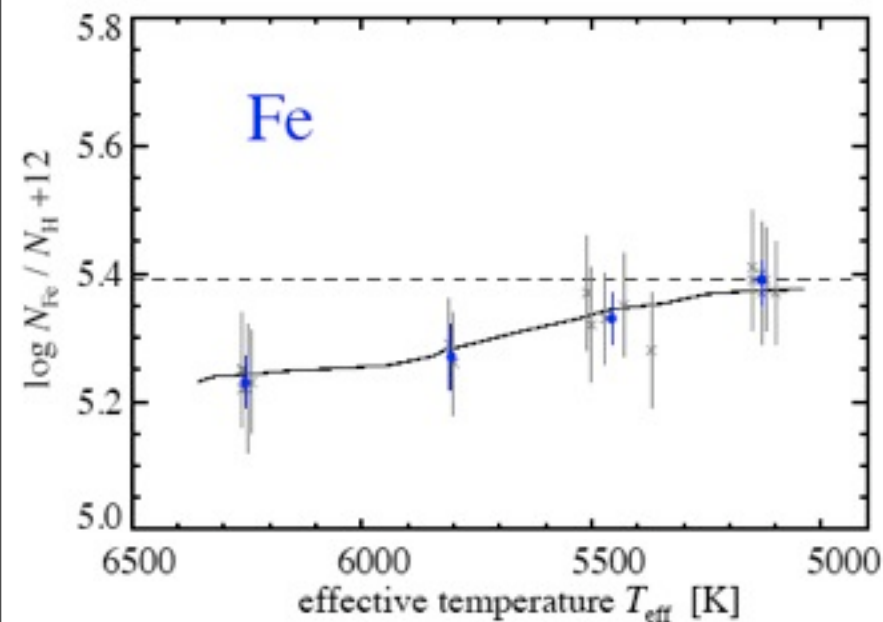
A Korn et al.

Figure 1: **Trends of iron and lithium as a function of the effective temperatures of the observed stars compared to the model predictions.** The grey crosses are the individual measurements, while the bullets are the group averages. The solid lines are the predictions of the diffusion model, with the original abundance given by the dashed line. In *b*, the grey-shaded area around the dotted line indicates the 1σ confidence interval of CMB + BBN[1]: $\log[\varepsilon(\mathrm{Li})] = \log(N_{\mathrm{Li}}/N_{\mathrm{H}}) + 12 = 2.64 \pm 0.03$. In *a*, iron is treated in non-equilibrium[20] (non-LTE), while in *b*, the equilibrium (LTE) lithium abundances are plotted, because the combined effect of 3D and non-LTE corrections was found to be very small[29]. For iron, the error bars are the line-to-line scatter of Fe I and Fe II (propagated into the mean for the group averages), whereas for the absolute lithium abundances 0.10 is adopted. The 1σ confidence interval around the inferred primordial lithium abundance ($\log[\varepsilon(\mathrm{Li})] = 2.54 \pm 0.10$) is indicated by the light-grey area. We attribute the modelling shortcomings with respect to lithium in the bRGB and RGB stars to the known need for extra mixing[30], which is not considered in the diffusion model.

Another way to determine the amount of ^{7}Li destroyed in stars is to observe the element's other, less stable, isotope: ^{6}Li. ^{6}Li is not made in detectable quantities by BBN but instead comes from spallation: collisions between nuclei in cosmic rays and in the interstellar gas. Since ^{6}Li is even more easily destroyed than ^{7}Li, detecting it allows us to place limits on the destruction of ^{7}Li.

In 2006 Martin Asplund and co-workers at the Mount Stromlo Observatory in Australia made extensive observations of ^{6}Li in plateau stars using the VLT. In each of the nine stars where they found ^{6}Li, roughly 5% of the lithium consisted of this isotope – which was larger than expected although at the limit of what was detectable with the equipment. This has huge implications not only for BBN but also for the history of cosmic rays in the galaxy and for stellar astrophysics. For example, the production of such large amounts of ^{6}Li must have required an enormous flux of cosmic rays early in the history of our galaxy, possibly more than could have been provided by known acceleration mechanisms. Moreover, if the plateau stars have truly destroyed enough ^{7}Li to bring the WMAP prediction of the mean baryon density into agreement with that obtained with the observed Spite plateau, the greater fragility of ^{6}Li implies that the stars initially contained ^{6}Li in quantities comparable to the observed ^{7}Li plateau.

All of these facts make the ^{6}Li observations an uncomfortable fit for BBN, stellar physics and models of cosmic-ray nucleosynthesis – particularly since the production of large amounts of ^{6}Li via cosmic rays has to be accompanied by a similar production of ^{7}Li. Although ^{6}Li can be produced in some exotic particle-physics scenarios, it is vital that we independently confirm Asplund's results. Indeed, the hunt for primordial lithium (of both isotopes) is currently ongoing at the VLT, as well as at the Keck Observatory and the Japanese Subaru Telescope, although such observations are right at the limit of what can be achieved.

Recent references on BBN and Lithium

M Asplund et al. 2006, "Lithium isotopic abundances in metalpoor halo stars" ApJ 644 229–259

T Beers and N Christlieb 2005, "The discovery and analysis of very metal-poor stars in the galaxy" Ann. Rev. Astron. Astrophys. 43, 531–580

A Korn et al. 2006 "A probable stellar solution to the cosmological lithium discrepancy" Nature 442, 657–659; 2007 "Atomic Diffusion and Mixing in Old Stars. I. Very Large Telescope FLAMES-UVES Observations of Stars in NGC 6397" ApJ 671, 402

C Charbonnel 2006, "Where all the lithium went" Nature 442, 636-637

K Nollett 2007, "Testing the elements of the Big Bang" physicsworld.com

R H Cyburt, B D Fields, K A Olive 2008, "An update on the big bang nucleosynthesis prediction for 7Li: the problem worsens" JCAP 11, 12 (also arXiv:0808.2818)

A J Korn 2008 "Atomic Diffusion in Old Stars --- Helium, Lithium and Heavy Elements" ASPC 384, 33
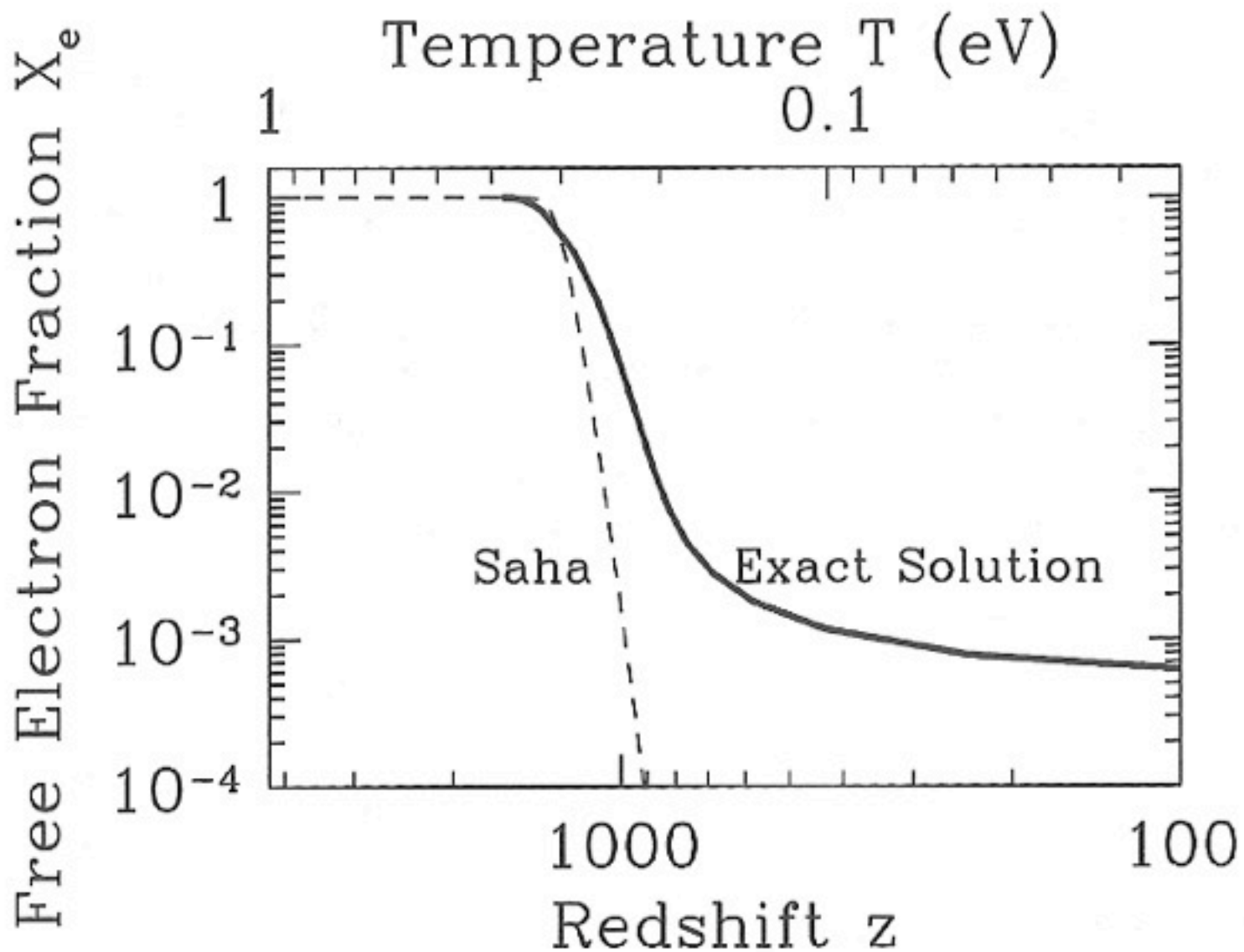
Figure 3.4. Free electron fraction as a function of redshift. Recombination takes place suddenly at $z \sim 1000$ corresponding to $T \sim 1/4$ eV. The Saha approximation, Eq. (3.37), holds in equilibrium and correctly identifies the redshift of recombination, but not the detailed evolution of X_e. Here $\Omega_b = 0.06, \Omega_m = 1, h = 0.5$.
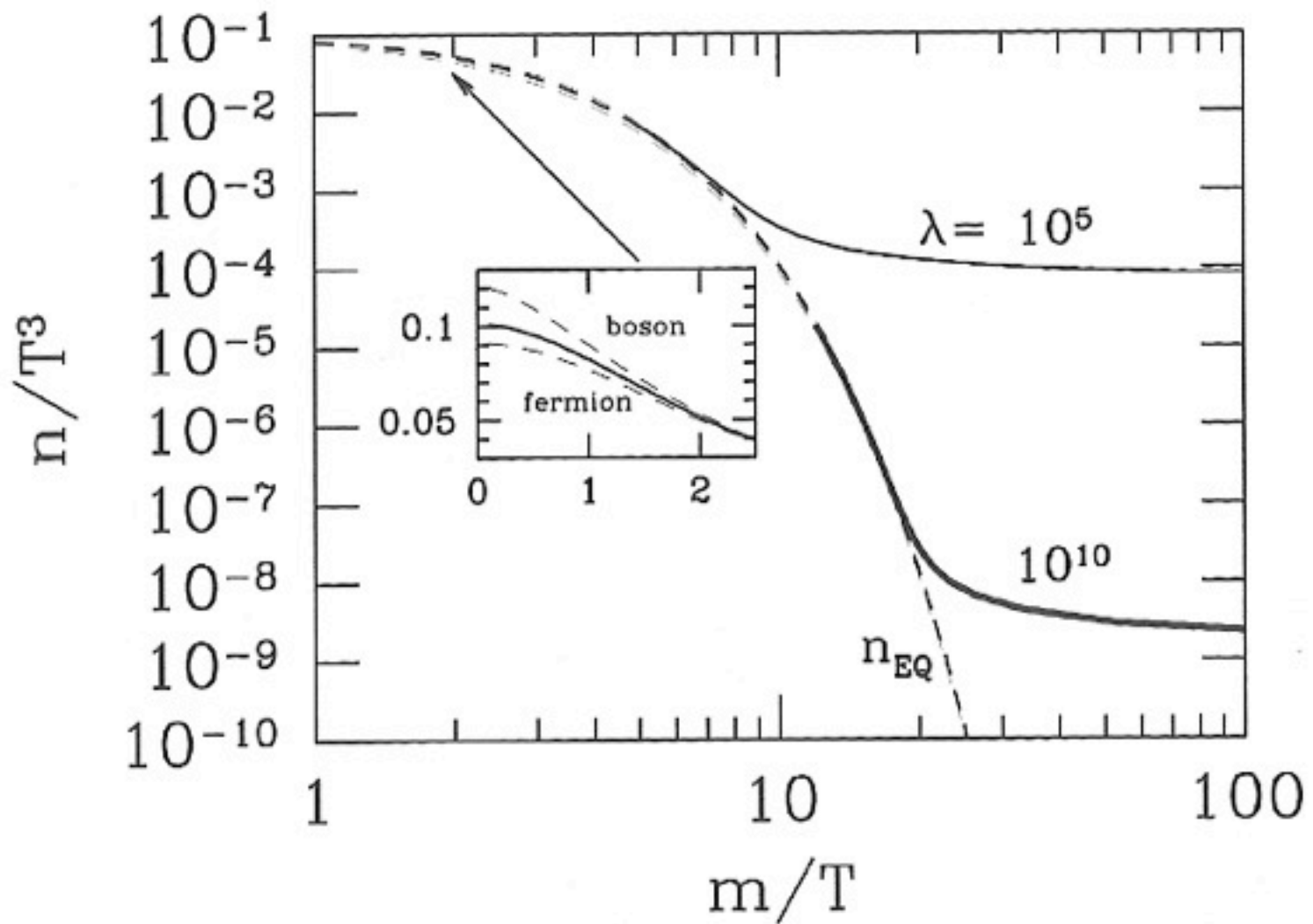
Dodelson, *Modern Cosmology*, p. 72

Figure 3.5. Abundance of heavy stable particle as the temperature drops beneath its mass. Dashed line is equilibrium abundance. Two different solid curves show heavy particle abundance for two different values of λ, the ratio of the annihilation rate to the Hubble rate. Inset shows that the difference between quantum statistics and Boltzmann statistics is important only at temperatures larger than the mass.

Dodelson, *Modern Cosmology*, p. 76